Investigation of solar cells sensitized with haematoxylin

دراسة عملية للخلايا الشمسية المحفزة بمادة الهيماتوكسيلين

Somya Kamal Abu Oun

Supervised by

Dr. Sofyan A. Taya
Associate Professor of Physics

Dr. Taher M. El-Agez
Associate Professor of Physics

A thesis submitted in partial fulfillment
of the requirements for the degree of
Master of Science in Physics

July, 2017

<div dir="rtl">

إقـــــرار

أنا الموقع أدناه مقدم الرسالة التي تحمل العنوان:

دراسة عملية للخلايا الشمسية المحفزة بمادة الهيماتوكسيلين

Investigation of solar cells sensitized with haematoxylin

أقر بأن ما اشتملت عليه هذه الرسالة إنما هو نتاج جهدي الخاص، باستثناء ما تمت الإشارة إليه حيثما ورد، وأن هذه الرسالة ككل أو أي جزء منها لم يقدم من قبل الآخرين لنيل درجة أو لقب علمي أو بحثي لدى أي مؤسسة تعليمية أو بحثية أخرى. وأن حقوق النشر محفوظة للجامعة الإسلامية – غزة.

</div>

Declaration

I hereby certify that this submission is the result of my own work, except where otherwise acknowledged, and that this thesis (or any part of it) has not been submitted for a higher degree or quantification to any other university or institution. All copyrights are reserves to IUG.

Student's name:	سمية كمال أبو عون	اسم الطالب:
Signature:	*Somya*	التوقيع:
Date:	18 أكتوير 2017	التاريخ:

نتيجة الحكم على أطروحة ماجستير

بناءً على موافقة شئون البحث العلمي والدراسات العليا بالجامعة الإسلامية بغزة على تشكيل لجنة الحكم على أطروحة الباحثة/ **سميه كمال حامد ابوعون** لنيل درجة الماجستير في كلية *العلوم* قسم *الفيزياء* وموضوعها:

دراسة عملية للخلايا الشمسية المحفزة بمادة الهيماتوكسيلين

Investigation of solar cells sensitized with hematoxyline

وبعد المناقشة العلنية التي تمت اليوم السبت 13 ذو القعدة 1438هـ، الموافق 2017/08/05م الساعة الحادية عشر صباحاً بمبني اللحيدان، اجتمعت لجنة الحكم على الأطروحة والمكونة من:

د. سفيان عبد الرحمن تايه	مشرفاً و رئيساً	....
د. طاهر محمد العاجز	مشرفاً	Taher M. E. Agm
د. وائل عبد طبازه	مناقشاً داخلياً	....
د. أمل محمود الكحلوت	مناقشاً خارجياً	....

وبعد المداولة أوصت اللجنة بمنح الباحثة درجة الماجستير في كلية العلوم/ قسم الفيزياء.

واللجنة إذ تمنحها هذه الدرجة فإنها توصيها بتقوى الله ولزوم طاعته وأن تسخر علمها في خدمة دينها ووطنها.

والله ولي التوفيق ،،،

نائب الرئيس لشئون البحث العلمي والدراسات العليا

أ.د. عبدالرؤوف علي المناعمة

Dedication

To my dear parents, Kamal & Hanan

To my lovely husband, Basel

To my daughter, Jana

Acknowledgment

First and above all, I acknowledge my thanks and praise to Allah, to granting me the capability to proceed successfully.

I would like to express my sincere thanks and gratitude to my supervisors Dr. Sofyan Taya and Dr. Taher El-Agez, they were always offers the guidance to go to the best.

Also I thank the professor of analytical chemistry in IUG Prof. Monzir Abdel-Latif.

I also thank my university and the staff members in Physics department at IUG for their continued support, a special mention for the support and assistance given by Mrs. Amal El-Batniji and Mr. Hatem El-Ghamri.

I thank my parents-in-law for their continuous support in all sides of my life.

And finally, I thank my family and all individual who has helped me during my study.

Abstract

The thesis presents the fabrication of dye sensitized solar cells based on dying titanium oxide with haematoxylin. The effects of many parameters on the cell performance were studied.

The optical properties of haematoxylin dye were studied using UV-Vis spectroscopy. The absorption spectra of haematoxylin dye dissolved in ethanol and water were studied and compered with haematoxyline dye on titanium oxide layer. Effect of dying time was also studied. pH number was changed using sodium hydroxide and hydrochloric acid. Adding copper and iron ions to haematoxylin dye dissolved in water and alcohol was studied and the performance of the cell was measured using (I^-, I^{-3}) redox and redox with sodium carbonate. It is found that the performance was improved when adding ions in alcohol medium. When adding sodium carbonate to the redox the performance of the cell was increased.

الملخص

نظراً لكون المشكلة العالمية الكبرى في يومنا هذا تتمثل في مشكلة الطاقة، وطرق توفيرها، والبحث عن سبل مختلفة للوصول إلى مصادر نظيفة ومتجددة للطاقة وبتكلفة محدودة، فكان تفكير الباحثين يتجه نحو دراسة الخلايا الشمسية الصبغية على الرغم من تعقيد بناءها.

يهدف هذا البحث إلى دراسة الخلايا الشمسية الصبغية المحفزة بمادة الهيماتوكسيلين باستخدام ثاني أكسيد التيتانيوم (TiO_2) كطبقة شبه موصلة، ودراسة تأثير العديد من العوامل المختلفة على كفاءة الخلية.

فقد تم دراسة تأثير زمن صبغ عينات الـFTO المدعمة بطبقة TiO_2 بصبغة الهيماتوكسيلين بتركيز $1*10^{-3}$ مولار ووجدنا أن أفضل نتيجة كانت عند زمن 20 دقيقة.

كما تم دراسة إضافة حمض الهيدروكلوريك وهيدروكسيد الصوديوم لتغيير الرقم الهيدروجيني لصبغة الهيماتوكسيلين ووجد أن الصبغة بوضعها الطبيعي تعطي أفضل كفاءة، فكان لإضافة الحمض والقاعدة لتغيير الرقم الهيدروجيني أثر سيء على كفاءة الخلية الشمسية.

وتم دراسة تأثير إضافة آيونات النحاس والحديد إلى صبغة الهيماتوكسيلين المذابة بالماء تارة وبالكحول تارة أخرى وقياسها باستخدام الريدوكس بدون إضافات وقياسها بإضافة كربونات الصوديوم (Na_2CO_3) إلى الريدوكس، ووجدنا تحسنا ملحوظاً عند إضافة الآيونات في وسط الكحول وتحسنا أكبر مع الريدوكس المضاف إليه كربونات الصوديوم خاصة عند إضافة الآيونات إلى الصبغة.

Table of Contents

List of Figures

List of Tables

List of Abbreviations

AM	Air mass
AM0	Air mass reference spectrum
AM1.5	Air mass 1.5 global spectrum
α	incident angle of light
PV	Photovoltaic
Si	silicon
Mono c-Si	Monocrystalline
Poly c-Si	Polycrystalline
sc-Si	Single crystalline silicon
mc-Si	Multi-crystalline Silicon
a-Si	Amorphous silicon
Cd-Te	Cadmium Telluride
CIS	Copper-Indium-Selenide
CIGS	Copper-Indium-Gallium-Diselenide
c-Si	Crystalline silicon
DSSC	Dye sensitized solar cell
CPV	Concentrating photovoltaic
TiO_2	Titanium dioxide
n-side	Negative side
p-side	Positive side
E_B	Energy barrier
E_P	Photo voltage
I_o	The intensity of the reference beam
V_{oc}	Open circuit voltage

I_{sc}	Short circuit current
J_{sc}	Short circuit current density
V_m	Maximum voltage
I_m	Current at the maximum power point
FF	Fill factor
P_m	Maximum power
I–V	Current – Voltage
J-V	Current density – Voltage
η	Solar energy to electric power conversion efficiency
P_{light}	energy of the light shining on the solar cell
R_s	Series resistance
R_{sh}	Shunt resistance
TCO	Transparent conducting oxide
ITO	Indium-doped tin oxide
FTO	Fluorine-doped tin oxide
eV	Electron volt
ZnO	Zinc oxide
SnO_2	Tin oxide
I^{-3}	Tri-iodide
I^-	Iodide
Pt	Platinum
HOMO	Highest occupied molecular orbital
LUMO	Lowest unoccupied molecular orbital
S	Oxidized state of the sensitizer
h	Plank's constant
S^*	Excited energy state of the sensitizer
e^-	Electron

$I - V$	Current-voltage
PV	Photovolatic
$J - V$	Current density – Voltage
$UV - Vis$	Ultraviolet-Visible
UV	Ultraviolet
T	Transmittance
I	Light intensity
A	Absorbance
λ_{max}	Maximum wavelength
IPA	Isopropyl alcohol
pH	potential of hydrogen
HCl	Hydrochloric acid
NaOH	Sodium hydroxide
N719	Bis(tetrabutylammonium)cis-di(thiocyanato)bis(2,2′ Bipyridine-4-COOH,4′
eV	Electron volt
AgCl	Silver chloride
N_2	Nitrogen gas
E_{ox}	Oxidation energy
E_{red}	Reduction energy
E_g	Energy bandgap
CV	Cyclic voltammetry
KOH	Potassium hydroxide
M	Molar

$CuSO_4$ Cupric sulfate

$FeSO_4$ Ferrous sulfate

Na_2CO_3 Sodium carbonate

Thesis layout

The thesis was arranged into four chapters.

- Chapter one presents the introduction, general overview of photovoltaic technologies and parameters of DSSCs.

- Chapter two presents an operating principle of DSSC and its components.

- Chapter three describes the experimental techniques used in this work and the experimental procedure.

- Chapter four presents all the results.

Chapter 1
Introduction

Chapter 1

Introduction

In this chapter, an introduction of solar cells is presented with the classification of energy sources. The solar radiation and air mass are also illustrated. The generations of photovoltaic solar cells and photovolatic processes in a solar cell are presented.

1.1 Energy Problem

The main concern of energy consumption through the world is the rapid depletion of fossil fuel, which are the three main elements used for energy production such as coal, oil, and natural gas. Fossil fuel is not environment friendly. This encourages scientists to search for alternative energy sources which are clean, inexhaustible and environment friendly, such as solar and wind energies. The usage of alternative energy sources has been set under attention; therefore, more than one alternative energy sources have been developed. Solar energy is the perfect source that has been selected among all the used sources. Producing electricity by solar energy has proved its maturity, reliability and efficiency, through the past two decades. Solar energy has been used in photovoltaic systems to produce electrical energy to satisfy consumer needs. Different methods have been adopted by scientists, in order to have better methods of solar radiation usage (Zghal, Kantchev, & Kchaou, 2012).

1.2 Classification of energy sources

Energy sources are classified into two types, non-renewable and renewable sources.

1.2.1 Nonrenewable energy sources

More than 90% of the world's energy needs depend on the underground storage of fossil fuels that are formed over millions of years and are threatened at any time and can't be replenished in a short period of time. To what extent can the world rely on this type of energy that is threatened with extinction at any time in the face of increasing demand for energy, as well as the harmful effects of the huge environmental and

economic consumption that is threatening the future humanity, from here, it was necessary to search for renewable and clean sources of energy to ensure the preservation of the future and the environment.

1.2.2 Renewable energy sources

Renewable energy can be obtained from natural resources which constantly replenished, such as wind, hydropower and solar etc. Renewable energy sources have the potential to meet the rising energy demand, and are expected to play an essential role in moving the world to a more secure, reliable and sustainable energy systems.

1.3 Solar Radiation and Air Mass

Inside the sun hydrogen fuses into helium and this fusion produces million degrees, which is the energy source of the sun.

Gaseous surface of the sun is like a black body, and the amount of energy that reaches the earth from the sun depends on the amount of reactions that get inside this huge nuclear reactor and the distance between the sun and earth.

Solar radiation power outside the earth's atmosphere is equal to 1.367 kWm^{-2}, this is known as the solar constant (Winter, Sizmann, & Vant-Hull, 2012).

Solar radiation passing through the atmosphere from the sun to the earth is absorbed and scattered partly. The ozone layer absorbs ultraviolet radiation and infrared radiation is absorbed by carbon dioxide and water vapor. Scattering of radiation occurs under the influence of particles, aerosols and clouds factors respectively, called Rayleigh, Mie and Cirrus scattering. The conditions of specific solar radiation are defined by the Air Mass (AM) value. Out of the atmosphere, spectral distribution and the total flux of radiation exhibits the behavior of black body of 6000°K, which have been defined as AM0.

The relative length of the path through the atmosphere by the shortest geometric path is given by:

$$AM = 1/\cos\alpha, \hspace{3cm} (1.1)$$

where α is the incident angle of light

The so-called AM1.5 conditions are achieved when the sun is at an angle of 41.8° above the horizon and results in the spectral distribution shown in Figure (1.1) and a solar flux of 963 Wm^{-2} (Corkish, Green, Watt, & Wenham, 2013).

Spectrum of Solar Radiation (Earth)
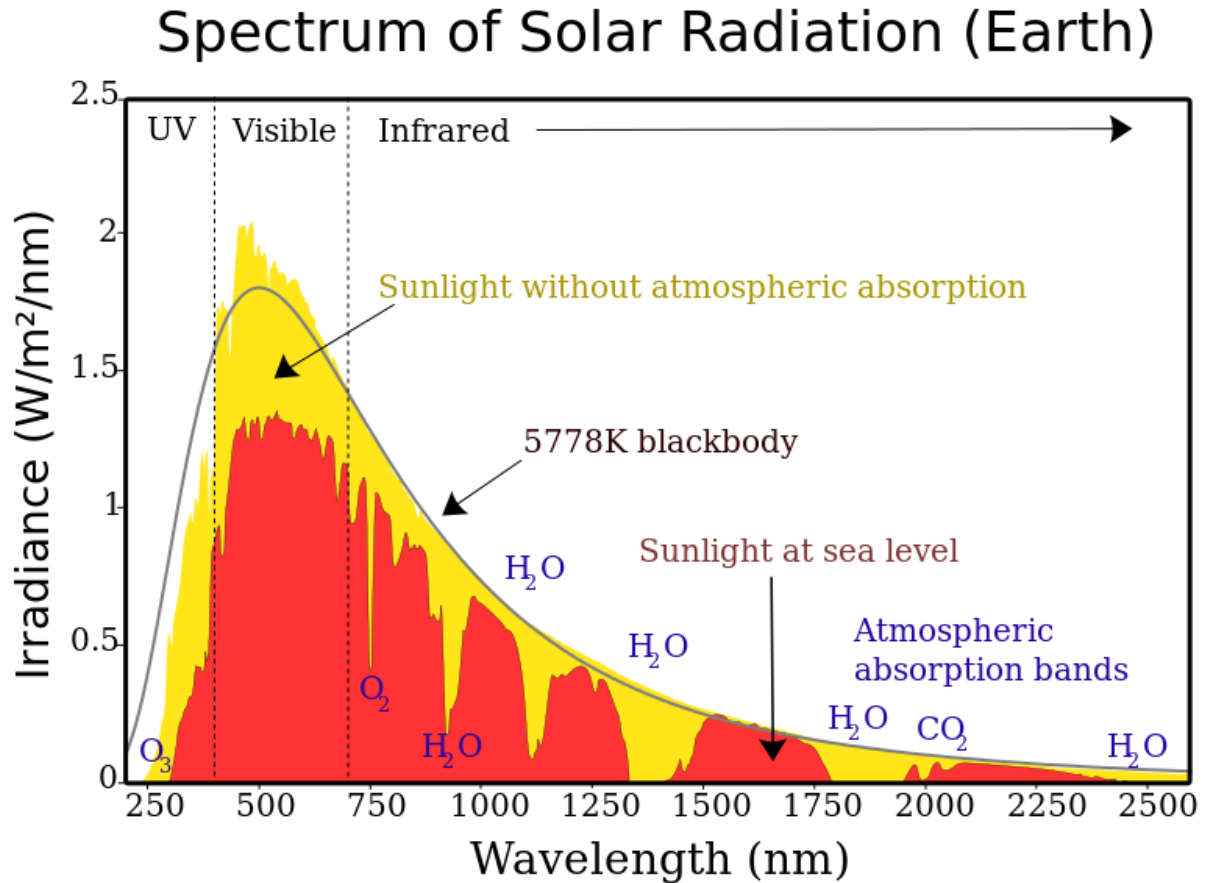
Figure (1.1): Spectral distribution of solar radiation.

1.4 Generations of Photovolatic Solar Cells

In 1839, Becquerel observed the photovoltaic (PV) effect, who mentioned a flow of current between two silver electrodes in an electrolyte media upon light exposure (Becquerel, 1839).

Solar cells can be classified into three generations.

1.4.1 First Generation of Photovolatic Solar Cells (1970s)

Silicon panels are the most common at the beginning of the emergence of solar cells. Silicon is the most common material in nature. According to Si wafers, there are two types of crystalline silicon cells are Monocrystalline (Mono c-Si) & Polycrystalline (Poly c-Si), which 90% of Photovoltaic cells depend on silicon variations

1.4.2 Second Generation of Photovoltaic Solar Cells (1980s)

The usage of crystalline silicon technologies to produce solar cells was expensive and needed more effort, but in the second generation, the usage of semiconductors to produce solar cells was cheaper in raw materials such as glass and flexible plastic.

There are three types of thin-film solar cells that have been commercially developed which are,

1. Amorphous silicon (a-Si)

Amorphous silicon is based on thin-film module prototypes which have the efficiency in the range of 7% to 15% (Green, Emery, Hishikawa, Warta, & Dunlop, 2013).

2. Cadmium Telluride (Cd-Te)

Cd-Te is a compound consisting of cadmium and tellurium elements. Cd and Te together as a compound is less toxic than Cd element. Compared to amorphous silicon, Cd-Te thin-film has a higher efficiency which is 15.8%, and lower production costs. It is concluded that the Cd-Te is more economical than amorphous silicon (Britt & Ferekides, 1993).

3. Copper Indium Selenide (CIS) and Copper Indium Gallium Diselenide (CIGS)

CIS & CIGS thin film of photovoltaic cells, have the highest efficiency of all PV technologies, which is between 7% to 16%, but efficiencies of up to 20.3% can be achieved in the laboratory (GREENY, Emery, Hishikawa, & Warta, 2011).

1.4.3 Third Generation of Photovoltaic Solar Cells (1990s)

The third generation is characterized by its low cost of materials, easy production, and higher efficiency.

Third generation involved three major techniques for producing solar cells:

1- Photovoltaic Technology

Photovoltaic technology is the first technique for producing solar cells, which is based on using optical devices, such as lenses, mirrors or other reflecting plates to concentrate direct sun light into solar cells plates. In PV technology, the solar cells plates have to be permanently oriented towards the sun, in order to obtain maximum performance for the plates. PV silicon based cells have efficiencies up to 20-25%, whereas PV based on multi-junction solar cells using III-V semiconductors have achieved efficiency of more than 40% in laboratory (Cotal et al., 2009).

2- Dye Sensitized Solar Cells (DSSC)

DSSC is the second technique for producing electricity, which was developed by O'Regan and Grätzel. The advantage of this type of solar cell is its ease fabrication from cheap materials. The spectral response of stable semiconductor's wide band gab such as, TiO_2 sensitized with dye can be extended to a visible light. In this case, free charge carriers are generated by electron or hole injection from the excited dye. The efficiencies of DSSCs are low, because there are very few dyes that can absorb a broad spectral range. In order to increase efficiency, a huge amount of organic dyes have been tested and studied to design and assemble nano structured materials. In the solid state DSSC, the efficiency increased from about 5% to over 15 % (Upadhyaya, Senthilarasu, Hsu, & Kumar, 2013).

3- Organic Solar Cells

Organic solar cells are the third technique for producing electricity, which consist of organic materials or polymers. Organic solar cells are characterized by its fabrication from cheap materials, flexibility and lightweight, but this technique had an efficiency range between 4% to 5% and 6% to 8% experimentally (Forrest, 2005).

4- Quantum Dot's Solar Cells

Quantum dots are semiconductor nanocrystals that exhibit unique optical properties due to a combination of their material band gap energy and quantum well phenomena.

When an electron is excited by a photon striking the quantum dot, it behaves as a particle confined in an infinite potential well, since the electron cannot escape from the quantum dot. The hole, created by the excited electron, behaves in the same fashion (Jones, Verlinden, & Quimby, 2007).

1.5 Photovoltaic Processes in a p-n Junction Solar Cell

Semiconductors consisting of p-n junction generate an electron-hole pair as shown in Figure (1.2). The electron will be drawn towards the n-side when it is illuminated by the light of suitable wavelength. The hole will be drawn towards the p-side of the p-n junction. Continuous radiation leads to reducing energy barrier (E_B) created by p-n junction which generates desired photo voltage (E_P). Eventually a steady-state condition will be reached between holes and electrons generated by light and their recombination. The band gap energy determines the maximum photovoltage that can be generated, which is called the open circuit potential, V_{oc}.
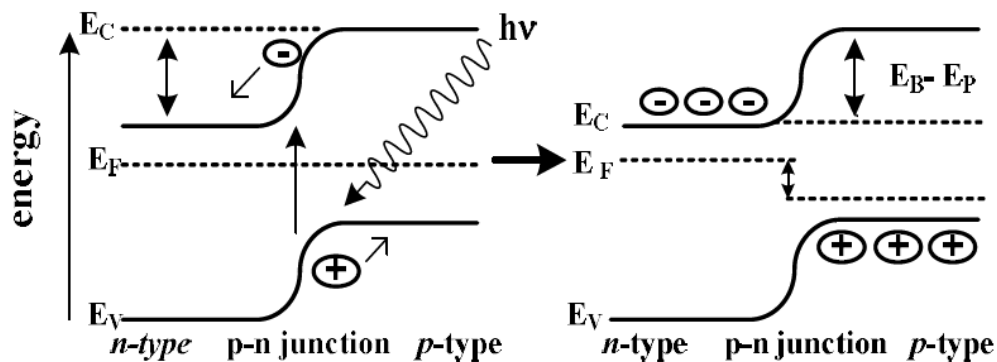
Figure (1.2): The p-n junction under illumination. Left: A photon induced hole-electron pair is separated by the local field of the junction. Right: The origin of the photo voltage E_P. E_B = Energy barrier created by the p-n junction, E_P = photo voltage.

1.6 Parameters of Solar Cells

There are a number of parameters that explain the solar cell work. These parameters are open circuit voltage, short circuit current, optimum voltage, optimum Current, fill factor, efficiency, and parasitic resistances, as shown in Figure (1.3).
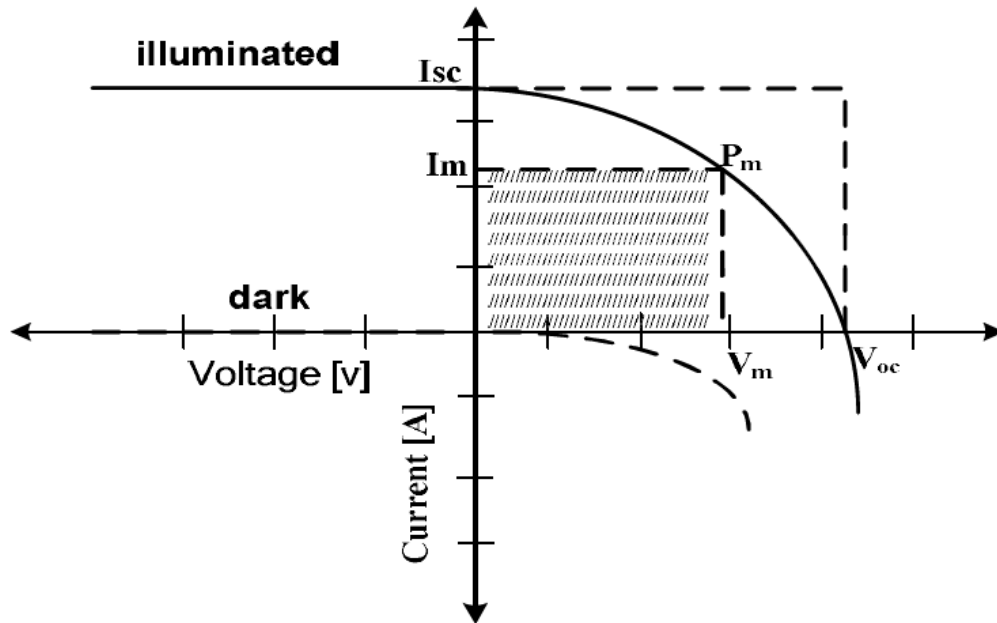
Figure (1.3): Voltage−current characteristics of a solar cell. Shaded area represents the maximum achievable output power.

a. Open Circuit voltage, V_{oc}

The open circuit voltage is obtained when no current is drawn from the solar cell.

b. Short Circuit Current, I_{sc}

It is the current obtained if the solar cell is short circuit and no potential differences across the cell.

c. Optimum Voltage, V_m

V_m is the voltage at optimum operating point at which the output power of the solar cell is maximum.

8

d. Optimum Current, I_m

I_m is the current at the optimum operating point.

e. Maximum output power, P_m

P_m is the multiplication of optimum current I_m and optimum voltage V_m.

f. Fill Factor, FF

Figure (1.3) illustrates the fill factor of a solar cell. It is the ratio between the shaded area of $V_m I_m$ and $V_{oc} I_{sc}$ which is:

$$FF = I_m V_m / I_{sc} V_{oc} \qquad (1.4)$$

Theoretically, higher open circuit potential higher value of fill factor.

g. Efficiency, η

The efficiency of solar cells is the ratio of the electrical energy output to the energy input from the sun. When power delivered to the load is P_{max}, maximum efficiency will be reached. Incident optical power is normally specified as the solar power on the surface of the earth which is approximately $1mW/mm^2$(Nelson, 2003). Maximum efficiency may be written as:

$$\eta = FF.I_{sc}.V_{oc} /P_{light}, \qquad (1.5)$$

where P_{light} is the energy of the light shining the solar cell and is obtained when the light intensities of the whole spectral range are integrated.

When increasing P_{light}, I_{sc} will be increased, but V_{oc} and efficiency of solar cells will be increased logarithmically (G Wolfbauer, 1999).

The four quantities: I_{sc}, V_{oc}, FF and η are the key performance characteristics of a solar cell.

9

h. Parasitic Resistances

In real cells, there is power dissipation through the resistance of the contacts and through leakage currents around the sides of the device. These effects are equivalent electrically to two parasitic resistances one is in series (R_s) and the other is in parallel (R_{sh}) with the cell as shown in Figure (1.4).
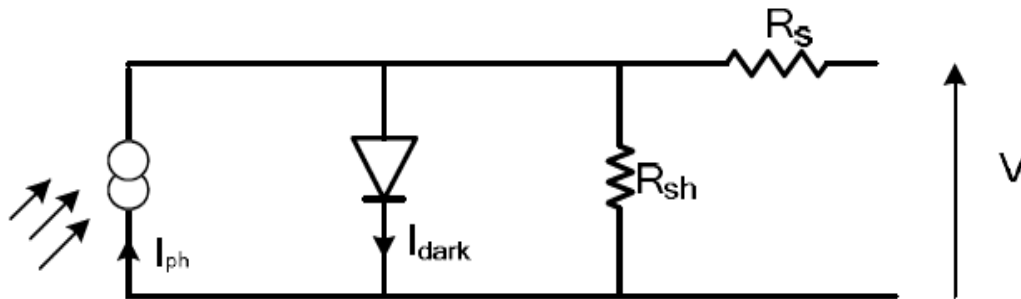
Figure (1.4): Equivalent circuit including series and shunt resistances.

1.7 Research Aims

Investigation of solar cells sensitized with haematoxylin dye using titanium dioxide (TiO_2) as a semiconducting layer, including many parameters such as dying time, changing pH number and adding the ions on the dye.

Chapter 2

Dye Sensitized

Solar Cells

Chapter 2

Dye Sensitized Solar Cells

In this chapter, the structure, the components, and the operating principles of dye sensitized solar cells (DSSCs) will be presented.

2.1 Introduction

Grätzel developed a new type of solar cells in 1991, which was known as dye-sensitized solar cell (DSSC), or Grätzel cell. It represents a good alternative to the standard silicon cell.

Of the most important advantages of this type of technology is the use of molecules to absorb photons, suitability for many of the materials, the possibility of production under mild conditions, and low cost.

2.2 Structure of DSSCs

In order to fabricate DSSCs, a sandwich configuration of two pieces of conducting glass is needed. Figure (2.1) shows the construction of a DSSC. It consists of substrate, TiO_2 semiconductor, sensitizing dye, electrolyte, the counter-electrode and electrical counter.
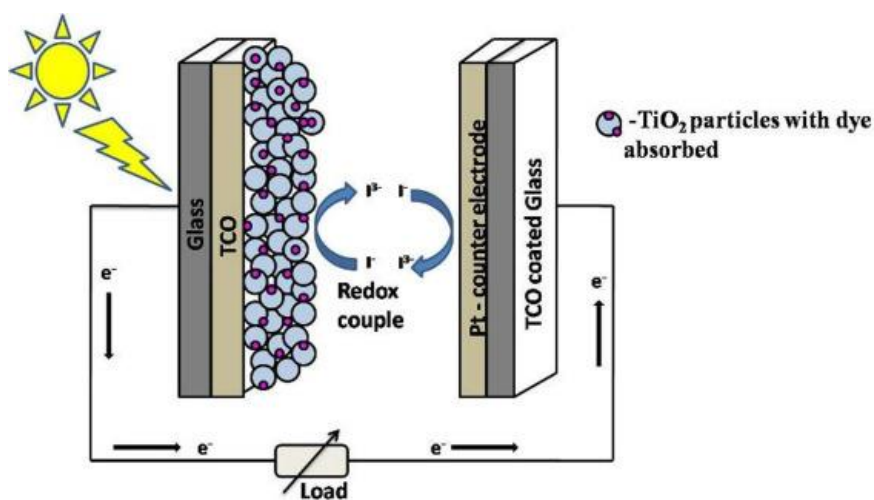
Figure (2.1): Construction of a DSSC.

2.2.1. Substrate

In DSSC, transparent conducting oxide (TCO) plated glass substrates are used to prepare electrodes. The cell is assembled between these substrates in order to prevent the entry of impurities such as water and oxygen to the cell. Low sheet resistance is needed for DSSC substrates, and it should be independent of temperature, up to 450 – 500 ^{o}C, and high transparency also is needed. Both the Indium-doped tin oxide (In:SnO$_2$, ITO) and fluorine doped tin oxide (F:SnO$_2$,FTO) form TCOs. In addition, the resistance of TCOs' sheet is around 10 Ω/cm^2. However, FTO glass is a better conducting substrate for the application in DSSCs this is because of ITO layers' poor thermal stability (Toivola, 2010).

2.2.2. TiO$_2$ Semiconductor

Semiconductors are materials where chemical doping is active to produce the charge carriers. There are two bands to distinguish intrinsic semiconductors: an empty conduction band, and a completely occupied valence band. On the other hand, the band gap is smaller than the energy of intrinsic absorption of photons. The intrinsic absorption of photons produces electron-hole pairs. In DSSCs, the large band gap (>3eV) metal oxides are used. Visible light cannot be absorbed by stable metal oxides because of their relatively large band gaps. There has been extensive studies on the sensitization of large band gap metal oxides, such as TiO$_2$, ZnO, and SnO$_2$, with photo sensitizers, such as organic dyes, natural dyes, that can absorb visible light; these studies were related to the development of photography technology since the late nineteenth century (Luque & Hegedus, 2011).

In this thesis TiO$_2$ was used which is the naturally occurring oxide of titanium. It has molar mass of 79.86g/mol, boiling point of 2972°C, melting point of 1843°C and refractive index of 2.488.

2.2.3. Sensitizing Dyes

The absorption of incident light in the DSSCs is realized by specifically engineered dye molecules placed on the semiconductor electrode surface. To achieve a

light of high energy conversion efficiency in the DSSC, the properties of the dye molecule as attached completely to the semiconductor surface. Such properties can be summarized as:

1- Energetics: To maximize the photo-voltage, the excited state of the adsorbed dye molecule shouldn't excessively exceed the conduction band edge of the TiO_2; instead, it should go slightly above in a degree that would contribute in the electron injection process by constituting an energetic driving force. Moreover, and for the same reason, the ground state of the molecule should be only slightly below the redox potential of the electrolyte.

2- Absorption: The dye should absorb light at wavelengths up to about 920nm, i.e. the energy of the exited state of the molecule should reach about 1.35eV above the electronic ground state corresponding to the ideal band gap of a single band gap solar cell.

3- Stability: the adsorbed dye molecule should achieve a proper stability level appropriate to the working environment (at the semiconductor-electrolyte interface) so that about 20 years of operation at exposure to natural daylight, i.e. at least 10^8 redox turnovers will be sustained.

These are the prerequisites for a proper photovoltaic sensitizer.

Nonetheless, the factors contribute to the process of dye-sensitization and that can yield good photovoltaic performance in the practical cell are more complicated in relation to all the partially unknown details now. It is not preferred to absorb light by other cell components such as the TiO_2 and the electrolyte for two reasons. First, it does not lead to current generation and reduces thereby the efficiency; second, it may induce side reactions with possibly degrading effects on the cell performance in the long term (Halme, 2002).

2.2.4. Electrolytes

The electrolyte used in the DSSCs generally consists of tri-iodide (I^{-3}) and iodine (I^-) as a redox couple in a solvent. There are possibly other substances added to improve the properties of the electrolyte and the performance of the operating DSSC.

The ideal characteristics of the redox couple are the following (Georg Wolfbauer, Bond, Eklund, & MacFarlane, 2001):

1- High solubility to the solvent for ensuring high concentration of charge carriers in the electrolyte.

2- Absence of significant spectral characteristics in the visible region to keep incident light away from absorption in the electrolyte.

3- High diffusion coefficients in the used solvent for enabling efficient mass transport.

4- Redox potential thermodynamically (energetically) proper with respect to the redox potential of the dye to maximize voltage cells.

5- Stable reduced and oxidized forms the couple so that long operating life will be enabled.

6- Chemical inactivity towards DSSC's components.

7- Highly reversible couple to facilitate fast electron transfer kinetics.

The following are the criteria for an appropriate solvent that would sustain a high efficiency liquid electrolyte DSSC (Stanley, Verity, & Matthews, 1998):

1- The solvent must be liquid and its volatility level must be low; i.e. at the operating temperatures (40°C - 80°C) so that the electrolyte wouldn't freeze or expand, or else the cells would be damaged.

2- The solubility of the intended redox couple in the solvent.

3- The dissolution of the redox couple should be facilitated by its high dielectric constant.

4- The rapid diffusion of charge carriers should be permitted by its low viscosity.

5- The sensitizing dye should not desorb into the solvent.

6- The cost and toxicity levels of the solvent should be low, as seen by the commercial production

7- It must be resistant to decomposition at the long term.

2.2.5. The Counter-Electrode

It consists of a conducting layer on a glass substrate. Often, a layer of platinum is coated on the substrate for the regeneration of the redox couple efficiently. The oxidized form corresponds to tri-iodide and its reduction involves two electrons in the case of the iodide/iodine redox couple. Moreover, it is necessary for the counter electrode to be catalytically active for the insurance of rapid reaction and low over potential. To avoid such problem, alternatives to platinum are needed. A prospective candidate is carbon. But platinum is a better catalyst for iodide/triiodide couple. Because (Pt) is a rare metal, therefore carbon (graphite) is used as a cheap alternative to platinum.

2.2.6. Electrical Contacts

This is similar to the amorphous silicon and the other thin film solar cells deposited on TCO coated glass; i.e. the limited conductivity of the TCO layer affects the design of dye cells and modules. To keep the reasonable low level of the resistive losses in the TCO layer, the longest distance from a photoactive point to a current collector should reach a maximum length of about 1 cm. For example, to fulfill this geometric requirement, the contact area of the current collector can be extended by using silver paint and adhesive copper tape. Alligator clips are easy to connect to these conductor strips in test cells. In case of attacking most metals (silver, aluminum, copper, nickel and gold), iodine based electrolyte is highly corrosive. This can make a problem when it comes to designing an electrical contacting of single cells in an integrated DSSC module.

2.3 Operating Principles

There is a difference between the DSSC and other solar cell types, and this difference appears by the basic construction of DSSC and the physical processes behind its operation. The typical DSSC configuration includes solid and liquid phases even though the 1st and 2ndgenerations of PV devices are based on solid semiconductor materials. The main difference to Si-based solar cells is the separation between charge generation (dye molecule) and charge-transport (TiO$_2$), and by the occurrence of charge

separation by means of kinetic irreversibility rather than by a built-in electrical field. Furthermore, there's a difference between initial photo excited species in organic molecules and those of silicon.

Generally, the operating mechanism of a DSSC is divided into 4 key basic steps:

1. Light absorption
2. Charge separation
3. Charge collection
4. Dye regeneration

Each of the interfacial electron transfer processes optimization is a major factor in the efficiency of the DSSC.

Figure (2.2) shows the simplicity of DSSC's basic operation. The critical idea is to make the light absorption process separated from the charge collection process, which encourages the combination of dye sensitizers with semiconductors, simulating natural light harvesting procedures in photosynthesis.
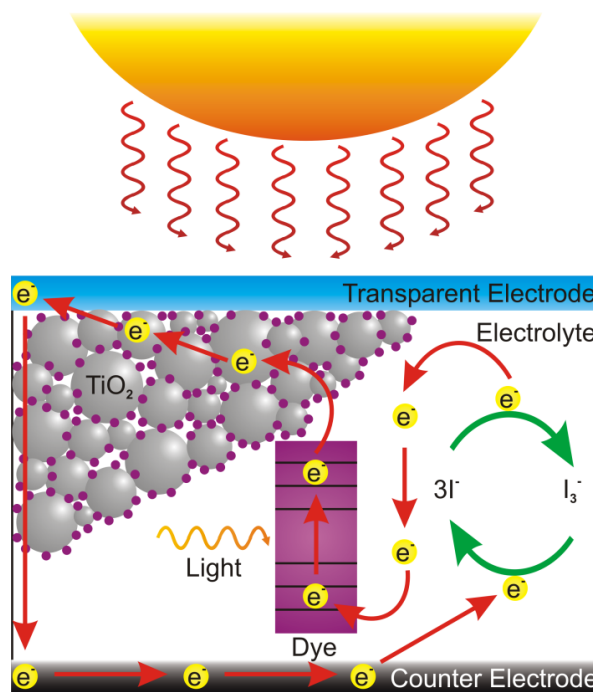
Figure (2. 2): Operation scheme of a dye sensitized solar cell ("Dye-sensitized solar cells: Best energy harvesting sources for future AF UAVs,").

Figure (2.2) shows the processes occurring throughout cell's operation, and they are briefly described below.

2.3.1 Light Absorption

The transparency of both the FTO layer with glass substrate, and the TiO_2 nano particles to visible light encourage photons of different energies in the sunlight to strike the cell, penetrating into the dye layer. Then, the dye absorbs the photon energy, which will promote one electron from highest occupied molecular orbital (HOMO) to lowest unoccupied molecular orbital (LUMO) if it is close to the energy gap of the dye molecule, which is the energy difference between the (HOMO) and (LUMO). The interfacial bonds between the dye and the TiO2 contribute to the injection of this excited electron from the excited state of the dye molecule into the conduction band of the semiconductor TiO_2. Equation 2.2 explains this process of the electron injection, which is one of the fastest known physical phenomena (Asbury et al., 1999) that occurs on the femtosecond scale. It is a crucial step because this is when the charge separation happens.

2.3.2 Electron Transport and Collection

Photo-injected electrons in the conduction band of the semiconductor are transported through the network by diffusion reaching FTO to generate electrical energy. The external load encourages the electrons to reach the counter electrode. Furthermore, the time scale at which the transport occurs is in the millisecond range.

2.3.3 Dye Regeneration

The oxidation of the dye molecule occurs after the electron injection., so it has to be consequently reduced, by the reduced form of the $redox$ mediator present in the electrolyte, in order to ensure the continuous operation of the device. Therefore, the oxidized dye molecules are regenerated by receiving electrons from the I^- ion redox mediator that becomes oxidized to I_3^- (Tri − iodide ions). After the electron injection, the oxidized dye should be reduced back to its original state as fast as possible in order to make the operating of DSSC efficient. The oxidized form of the redox mediator I_3^-

needs to be reduced and this takes place at the counter electrode, which substitutes the internally donated electron with that from the external load and reduced back to I^- ion. Thus, generation of electric power in DSSC causes no permanent chemical change or transformation from this cycle (Grätzel, 2005).

The following chemical reactions can summarize the operating cycle of DSSC:

Anode:

$$S + \mathrm{h}v \longrightarrow S^* \qquad\qquad \text{Photo-excitation of the dye} \qquad\qquad (2.1)$$

$$S^- \longrightarrow S^+ + e^- \quad (TiO_2) \qquad \text{Electron injection in TiO}_2 \qquad\qquad (2.2)$$

$$2S+ + 3I^- \longrightarrow 2S + I_3^- \qquad \text{Regeneration of the dye} \qquad\qquad (2.3)$$

Cathode:

$$I_3^- + 2e^-(Pt) \longrightarrow 3I^- \qquad\qquad \text{Reduction of the redox} \qquad\qquad (2.4)$$
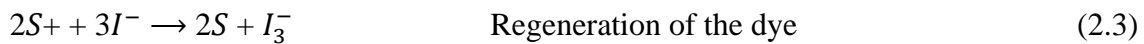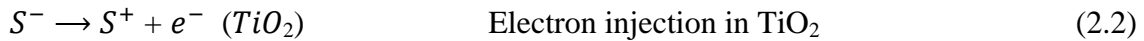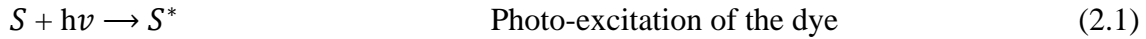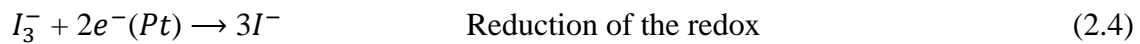
The main loss processes in a DSSC are summarized in these points:

1. Recombining the injected electron with the oxidized dye.
2. Losing the injected electron in the conduction band to the tri-iodide in the electrolyte (also known as the dark current).
3. Having the excited electron relaxed back to the ground state of the dye.

The kinetic competition between the various forward steps and the charge-recombination processes are major factors for the efficiency of charge separation and energy conversion.

2.3.4 Types dyes as sensitizers

DSSCs are based on natural and synthetic dyes. The use of natural dyes extracted from trees, fruits, and vegetables as sensitizers for the conversion of solar energy into electricity is very interesting because it improves the economical aspect and makes important profit from the environmental (Abdel-Latif, Abuiriban, El-Agez, & Taya, 2015).

Chapter 3

Research

Techniques

Chapter 3

Research Techniques

In this chapter, the techniques and materials used for the preparation of DSSC are discussed.

3.1 Experimental Techniques

The experimental techniques which used to characterize DSSCs are described. Current-voltage characterization can be obtained with a solar simulator. Testing the optical properties of the dye by ultraviolet-visible (UV-Vis) spectroscopy is presented.

3.1.1 Solar Cell I-V Measurement Systems

I-V measurement is used in solar cell performance measurements. The simulation system consists of a calibrated tungsten halogen lamp. Illuminated (I-V) characteristics of photo voltaic (PV) device is measured with respect to standard conditions, are defined by intensity, spectrum, area and temperature. For testing the solar cell, a source of light that simulate solar standard (AM1.5) is needed. To activate that system, a special program should be installed on the computer; it's known as Autolab NOVA software. NOVA is the data reading and analyzing software package for all Autolab functions. After measuring the I-V curves, the performance parameters of the cell, such as short circuit current (I_{sc}), open circuit voltage (V_{oc}), maximum current (I_{max}), maximum voltage (V_{max}), maximum power (P_{max}), fill factor (FF) and the efficiency (η) can be calculated.

I-V characteristic curve of the assembled DSSC was investigated by running the function linear sweep voltammetry potentiostatic in NOVA program, where the applied potential ranged from -0.7V to 0.7V.

Figure (3.1), shows the Autolab AUT 85276 Potentiostat- Gelvanostat together with the solar simulator used in all the I-V measurements.
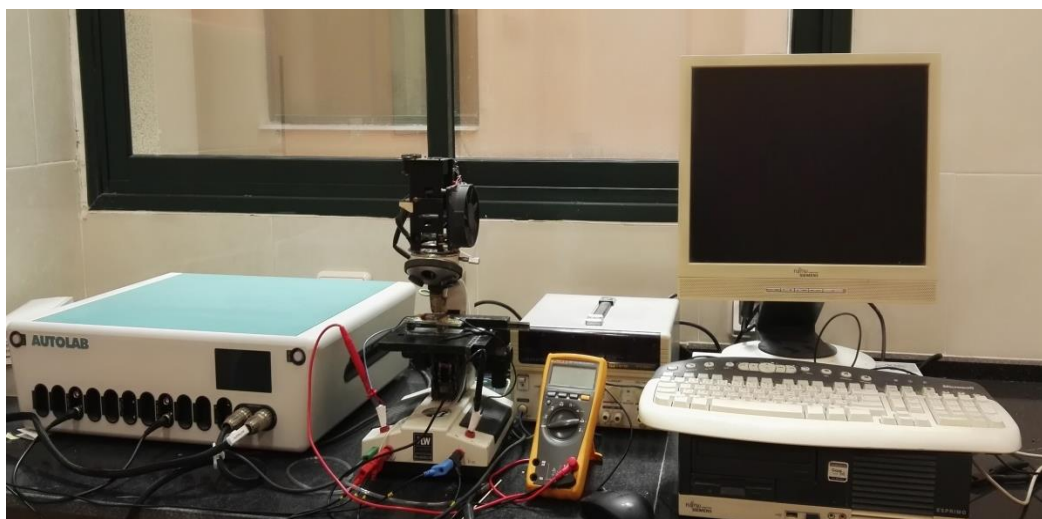
Figure (3.1): Autolab AUT 85276 Potentiostat- Gelvanostat and the solar simulator used in the measurements.

3.1.2 UV-Vis Spectroscopy

Ultraviolet and visible (UV-Vis) absorption spectroscopy is the measurement of the light beam's attenuation after reflection from a sample surface or after passing through a sample. Measurements of absorption can be at a single wavelength or over an extended spectral range.

The UV-Vis spectral range is approximately between 190 to 900 nm. The ultraviolet (UV) region scanned is normally from 200 to 400 nm, and the visible portion is from 400 to 700 nm. A beam of light from a visible or UV light source is separated into its component wavelengths by a prism or diffraction grating. Then, a half-mirrored device contributes to splitting each monochromatic beam in turn into two equal intensity beams. The sample cuvette, which contains a solution of the compound studied in a transparent solvent, crosses a small transparent container (cuvette), while the other, the reference cuvette, which contains only the solvent, passes through an identical cuvette. Then, electronic detectors measure and compare the intensities of these light beams (Rouessac & Rouessac, 2013). The intensity of the reference beam indicates no

22

light absorption (I_0). Knowing that (I) is used to define the light intensity beam in the presence of a sample.

The ratio I/I_0 which doesn't depend on the change of the intensity of incident light is called the transmittance

$$T = I/I_0 \qquad\qquad (3.1)$$

In regard to the definition of the absorption coefficient α for a uniform medium, we take into account the intensity change of a monochromatic light beam in a unit distance where that the beam travelled (Meyer-Arendt, 1989).

$$\frac{dI}{dx} = -\alpha I \qquad\qquad (3.2)$$

The beam intensity as a function of the distance x is, therefore, defined as this:

$$I = I_0 e^{-\alpha x} \qquad\qquad (3.3)$$

The definition of absorbance is given by

$$A = -\log T \qquad\qquad (3.4)$$

Transmittance (T) or absorbance (A) represents the absorption. In case of no absorption, T = 1 and A= 0.

Thus, it becomes clear that there's a proportional relationship between the absorbance and absorption coefficient.

If there's no absorption of light of a given wavelength by the sample compound, then $I = I_0$. On the other hand, I is less than I_0 if the sample compound absorbs light.

A theory of diffuse reflection at scattering surfaces was derived by Munk in 1931 and Kubelka 1948 describes optical characteristics. The Kubelka -Munk function is given as:

$$F(R) = \frac{(1-R)^2}{2R} = \frac{K}{S}$$ (3.5)

Where:

R = absolute reflectance of the layer

K= molar absorption coefficient

S= scattering coefficient

Our absorption spectra and Kubelka -Munk were recorded by THERMO EVOLUTION 220 UV-Visible spectrophotometer. The UV-Vis spectrometer used in this study is shown in Figure (3.2)

Figure (3.2): Thermo evolution 220 UV-Visible spectrophotometer.

3.2 Device Fabrication

In this section, DSSCs were prepared using haematoxylin dye extracted from the heartwood of the logwood tree.

3.2.1 Materials Used in the Preparing of DSSCs

a) Fluorine-doped Tin dioxide (FTO:SnO_2), conductive plates with sheet resistance of 15 Ω/cm^2 and transmission >80%.

b) TiO_2 nanoparticles with 10-25 nm.

c) Natural dyes of haematoxylin.

d) A redox (I^-/I^{-3}) electrolyte solution.

e) A counter electrode (Pt).

f) Electrical contact between working and counter electrodes is achieved by alligator clips.

3.2.2   Cleaning FTO Glass

The FTO conductive glass substrates with sheet resistance of 15 Ω/cm^2 and transmission >80% (Xinyan Tech. Ltd, Hong Kong) were cut into pieces of dimensions 1.6 cm x 1.6 cm.

The glass was cleaned in distilled water using an ultrasonic bath for 20 min by the Ultrasonic Cleaner shown in Figure (3.3), then sonicated in Isopropyl alcohol (IPA) for 5 min, rinsed thoroughly twice in water, sonicated in 10wt% NaOH solution for 5 min, rinsed with water and ethanol and dried in an oven at 60°C for 30 min. The sheet resistance of the FTO conductive glass was measured and found to be 15-30 Ω/cm^2.

Figure (3.3): Ultrasonic Cleaner.

3.2.3 Preparation of TiO₂ Electrode

The semiconductor paste was prepared by blending TiO_2 with polyethylene glycol with the rating of 1:2. As shown in Figure (3.4)**,** the thickness of the film should be controlled and the electric contact strips should be masked, so two edges of the FTO glass plate were covered with a layer of Adhesive tape. Successively, and through the sliding of a metallic rod along the tape, the TiO_2 paste was uniformly spread on the substrate, and a TiO_2 layer of area $0.25cm^2$ was obtained. As shown in Figure (3.5), and after spending 40 minutes in heating up the FTO glass with TiO_2 film to $450^{°}C$ in an oven , the sintering process was completed and the TiO_2 deposited- electrode was cooled down to $100^{°}C$. Afterwards, the samples were submerged in the heamatoxylin dye as will be explained in chapter 4.
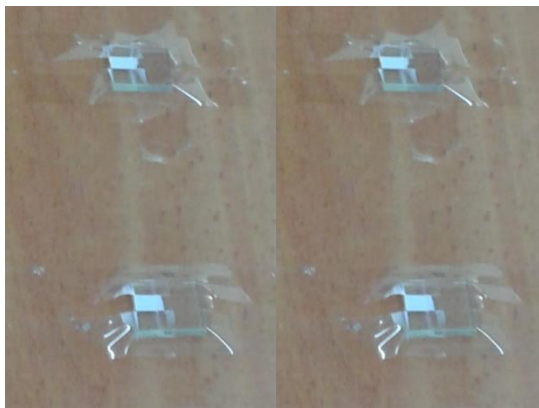
Figure (3.4): spearding the TiO_2 paste on the FTO coated glass.

Figure (3.5): An oven used in the sintering process.

3.2.4 Preparing liquid electrolyte

Liquid electrolyte was prepared by dissolving 0.66 gm of lithium iodide (LiI) and 0.63 gm of iodine (I_2) in a beaker containing 2ml of acetonitrile (ACN) and 8ml of propylene carbonate (p- carbonate). The solution was heated for 20 minutes on the hot plate with stirring, and then the electrolyte was kept in a black bottle to be used later in the DSSC device.

3.2.5 Haematoxylin dye

Haematoxylin, also called natural black 1 or C.I. 75290 with the chemical formula of $C_{16}H_{14}O_6$ is a compound extracted from the heartwood of the logwood tree. The molecular structure is presented in figure (3.6). It is the most commonly used stains in histology. To prepare a haematoxylin solution of concentration 1mM, 0.006 gm of the haematoxylin was dissolved in 20 ml of distilled water or ethanol. The prepared solution was used in dying TiO_2 films.
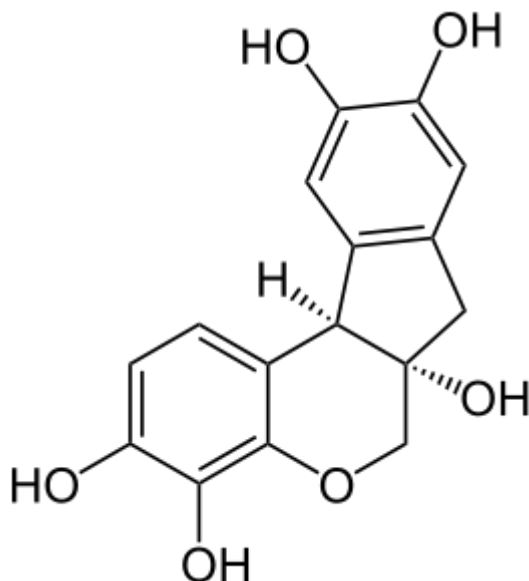
Figure (3.6): The molecular structure of haematoxylin dye.

3.2.6 Assembly of DSSC

Finishing fabrication of DSSCs, it is consist of dyed TiO_2 and platinized counter electrode. The two electrodes form a sandwich configuration, where the upper part is the dyed film (the anode) and the lower part is the counter electrode. They should be placed in a way that they are slightly offset in order to allow connections to the leads of the I-V measurement setup. Using micropipette, a tiny electrolyte redox (I^-/I_3^-) drop is placed between the two electrodes.

Chapter 4

Results & Discussions

Chapter 4

Results and Discussions

In this chapter, the experimental results will be discussed in details, including the J-V curves and the impact of some factors on the performance of the cell such as optimizing time of dying, influence of pH solution of the dye, and adding iron and copper ions.

4.1 Absorption Spectra and Kubelka-Munk of Haematoxylin Dye

The Absorption spectra of Haematoxylin dye solutions in ethanol and water as solvents were investigated using THERMO EVOLUTION 220 UV-Visible spectrophotometer. The absorption spectra analysis was carried out in the wavelength range from 300 to 800 nm as shown in Figure (4.1). As observed from the Figure, absorption peaks are found at 446 nm in both ethanol and water. It is also found that there is an extra peak at 556 nm in water. As shown in Figure (4.2) (a), in ethanol the absorption peaks are found at 446 nm and kubelka-munk peaks at 479 nm. Also from Figure (4.2) (b), in water the absorption peaks are found at 446 nm and kubelka-munk peaks at 487 nm. We note that there are shifts in the absorption peaks of 33 nm in ethanol and 41 nm in water. The longer of wavelength after soaking the TiO_2 electrode in the dye solution resulted from the interaction between the TiO_2 molecules with the dye.
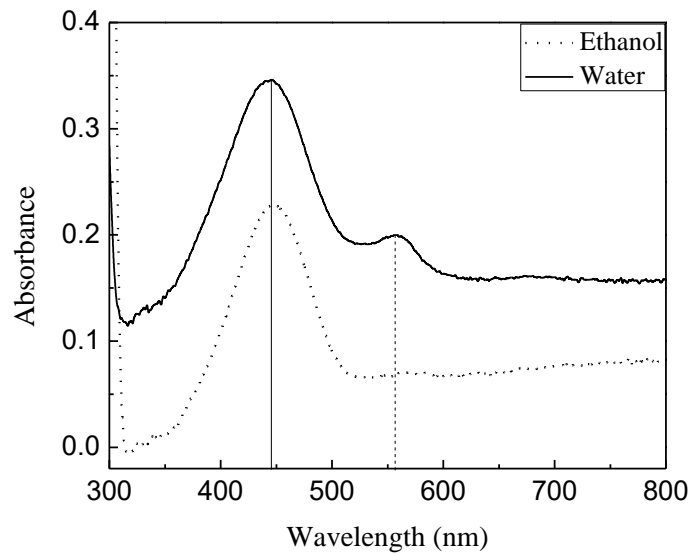
Figure (4.1): The UV–Vis absorption spectra of Haematoxylin dye solutions in ethanol and water.
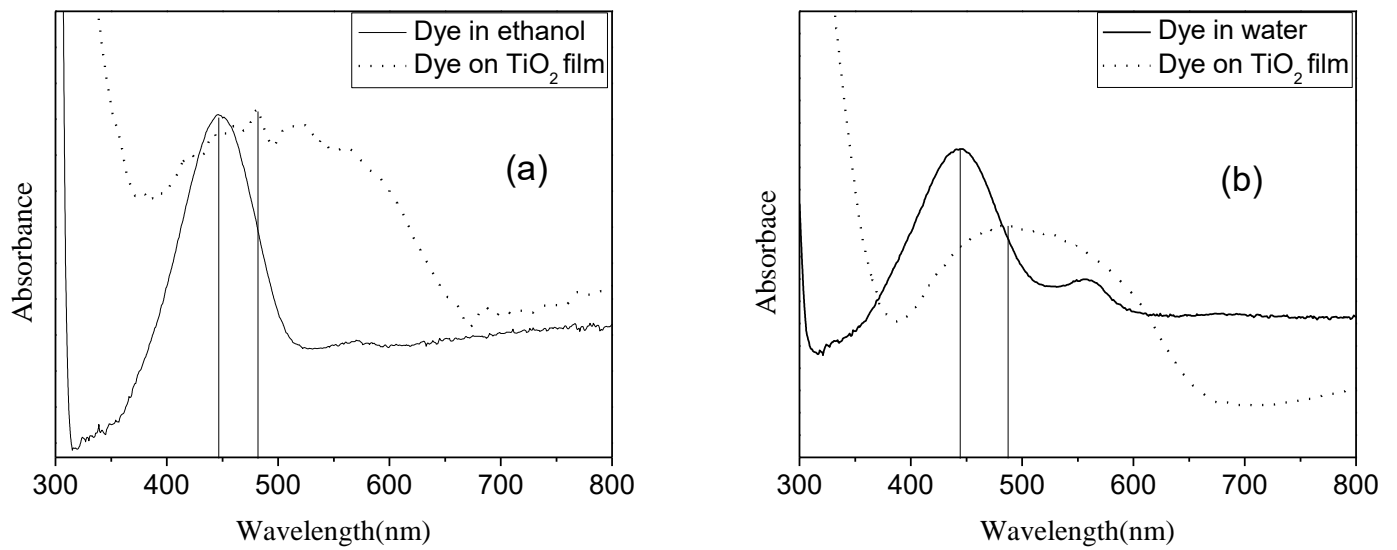
Figure (4.2): Kubelka-Munk and UV–Vis absorption spectra of Haematoxylin dye solutions in (a) ethanol, (b) water.

31

4.2 J-V Characterization of DSSCs Sensitized with Haematoxylin dye compared with Ru(N719)

Once the DSSC is fabricated, it is now important to evaluate its performance. The J-V characteristic curves of the DSSCs sensitized with Haematoxylin dye in ethanol at $1000W/m^2$ illumination and in the dark are shown in Figure (4.3). It is clear from the figure, the J-V curve in the dark looks like the diode curve. The J-V characteristic curves of the DSSCs sensitized with Ru (N719) dissolved in ethanol about one day, and Haematoxylin dye dissolved in ethanol about 15 minute at $1000W/m^2$ illumination as shown in Figure (4.4).

As shown in Figure (4.3) and Figure (4.4) the values of J_{sc} and V_{oc} can be obtained for all DSSCs directly using the J- V data. The maximum power point is determined from the power (P)-voltage (V) curves as shown in Figure (4.5) and Figure (4.6) from which J_m and V_m can be obtained. The fill factor and cell efficiency are calculated using Equation (1.4), $FF = I_m V_m / I_{sc} V_{oc}$, and Equation (1.5), $\eta = FF.I_{sc}.V_{oc} /P_{light}$ respectively. All the photovoltaic parameters of the fabricated DSSCs sensitized by Haematoxyline and Ru (N719) dyes are listed in Table (4.1).
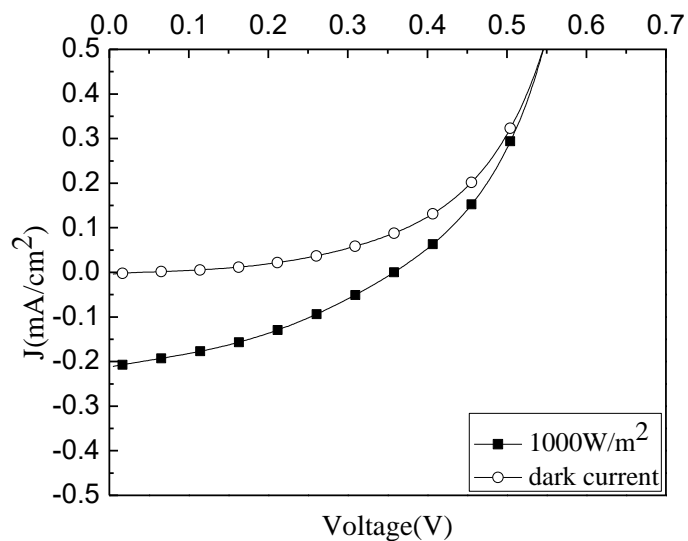
Figure (4.3): Current density (J) versus voltage (V) characteristic curves for the DSSCs sensitized by Haematoxylin dye at 1000W/cm^2 illumination and in the dark.
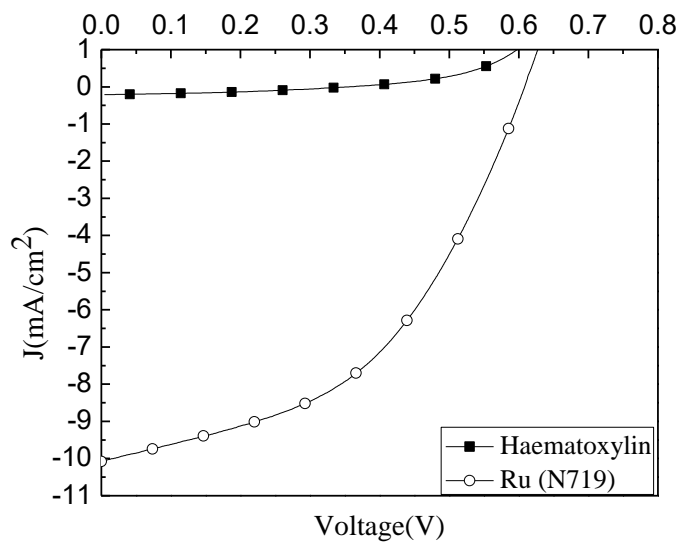
Figure (4.4): Current density (J) versus voltage (V) characteristic curves for the DSSCs sensitized by Haematoxylin dye and Ru (N719).
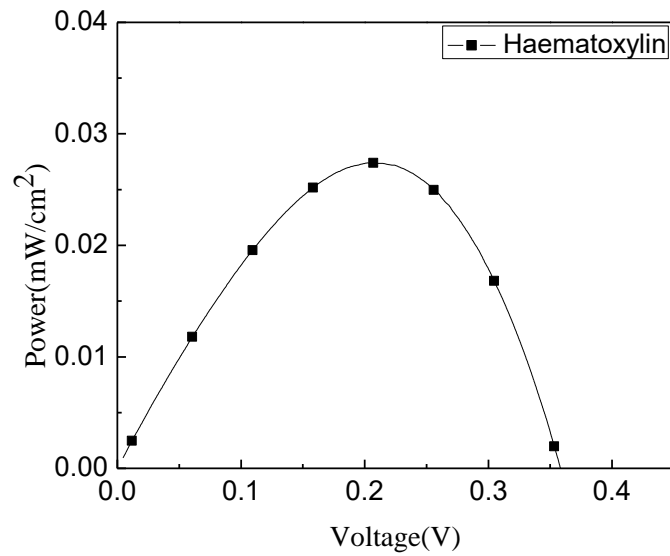
Figure (4.5): Power (P) versus voltage (V) characteristic curves for DSSC sensitized with Haematoxylin dye solutions.

Figure (4.6): Power (P) versus voltage (V) characteristic curves for DSSC sensitized with Ru(N719).

Table (4.1): Photovoltaic parameters of the DSSCs sensitized by Haematoxylin and Ru (N719) dyes.

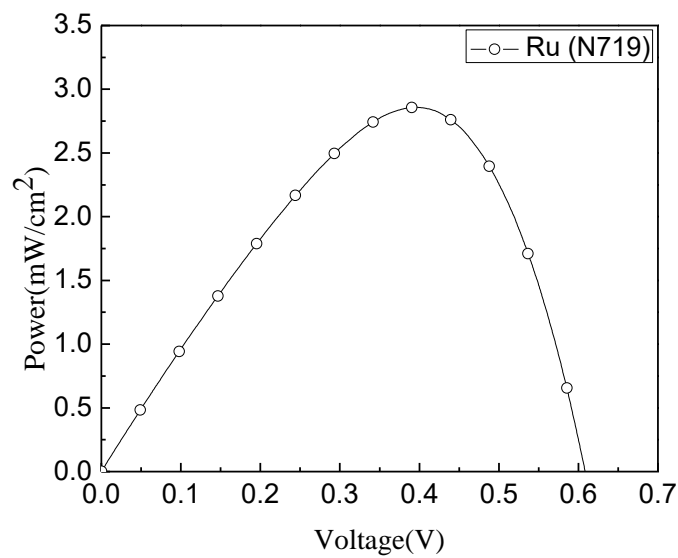| Dye	J_{sc} (mA/cm^2)	V_{oc} (V)	J_m (mA/cm^2)	V_m (V)	P_{max} (mwatt/cm^2)	FF	η %
Haematoxylin	0.21	0.36	0.13	0.21	0.027	0.35714	0.027
Ru	10.06	0.61	7.33	0.39	2.87	0.46769	2.87

4.3 Cyclic Voltammetry Potentiostatic (CV)

HOMO and LUMO levels can be determined using Auto lab as follow:

1- Putting the Heamatoxyline dye in the beaker and adding the calibration material with known energy gab on it, for example silver salts with energy gap of 4.4 eV.

2- Connecting the positive pole with platinum side.

3- Connecting the negative pole with another side (AgCl).

4- Connecting N_2 as shown in the Figure (4.7).

5- Perform the measurement process by the Auto lab and Figure (4.8) was obtained.

6- HOMO and LUMO Energy can be calculated using this equation

$$E_{HOMO} = -(4.4 + E_{ox})\ eV \tag{4.1}$$

$$E_{LOMO} = -(4.4 + E_{red})\ eV \tag{4.2}$$

$$E_g = E_{LOMO} - E_{HOMO} \tag{4.3}$$
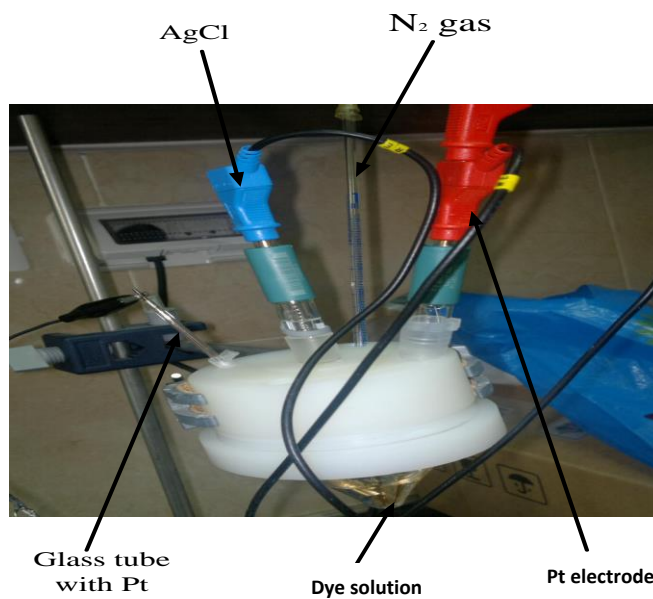
Figure (4.7): Connection poles to find HOMO and LUMO for the dye.
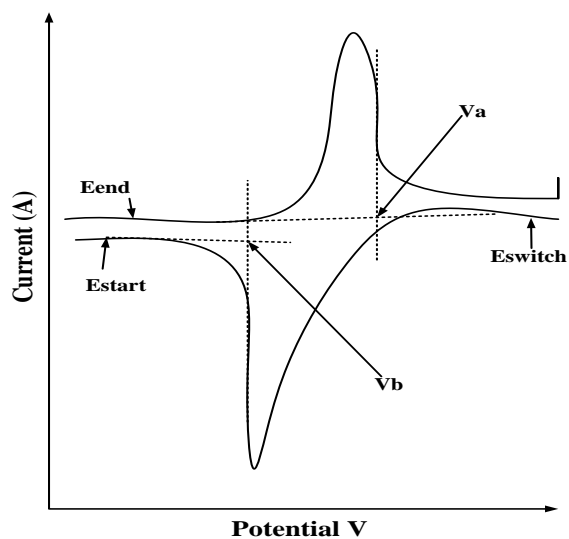
Figure (4.8): Standard Curve of Cyclic Voltammetry measurment.

The Cyclic Voltammetry (CV) was measured by Auto lab for Heamatoxylin dye as shown in Figure (4.9). The HOMO and LUMO Energy levels can be determined using Equations (4.1), (4.2) and (4.3). From Figure (4.9), we can find the oxidation energy $(E_{ox}) = 0.93\ eV$ and the energy band gap $(E_g) = 4.04\ eV$ from Figure (4.10). Then using equations (4.1), (4.2) and (4.3),

$$E_{HOMO} = -5.33eV \qquad \text{and} \qquad E_{LOMO} = -1.29\ eV.$$
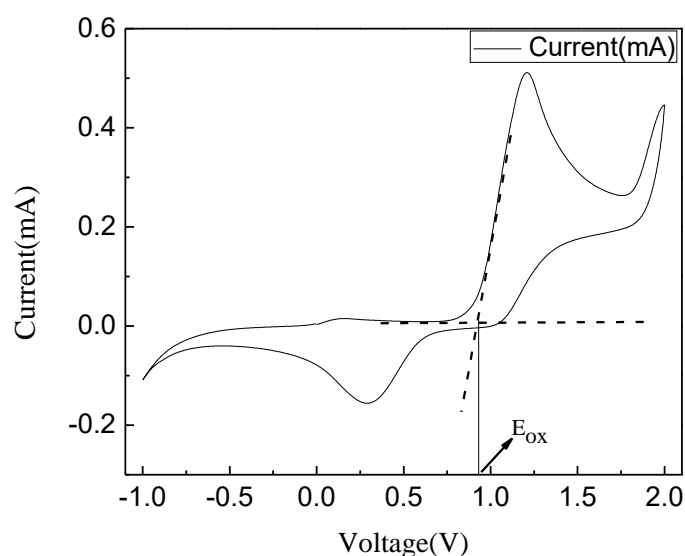
Figure (4.9): Cyclic Voltammetry (CV) of Haematoxylin dye.
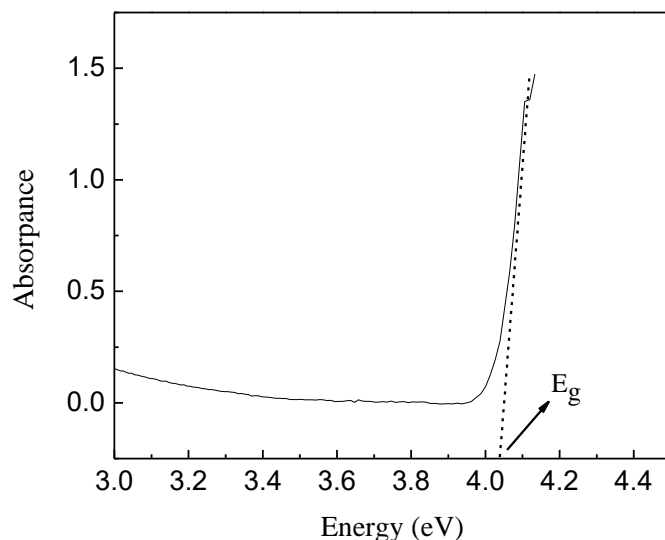
Figure (4.10): Energy band gap vs absorption with Haematoxylin dye.

4.4 Effect of dying time on DSSC Efficiency

To investigate the effect of the dying time on the performance of DSSC sensitized by Haematoxylin dye as photosensitizers, we select a time range from 15 minutes to one day. After Preparing $1 \times 10^{-3} molar$ of Haematoxylin dye solution in ethanol, FTO samples with titanium layer were placed in the dye solution at different times. The J-V characteristics of DSSCs sensitized with Haematoxylin dye at different dying time from 15 minute to one day are shown in Figure (4.11).

As shown in Figure (4.11) the values of J_{sc} and V_{oc} can be obtained for all DSSCs directly using the J-V data. The maximum power point is determined from the power (P)-voltage (V) curves as shown in Figure (4.12) from which J_m and V_m can be obtained. DSSC efficiency versus dying time curve as shown in Figure (4.13). All the photovoltaic parameters of the fabricated DSSCs sensitized by Haematoxyline dye at different dying times are listed in Table (4.2).

Based on the results in Table (4.2), it is noticed that the highest efficiency was obtained at 20 minute dying time.
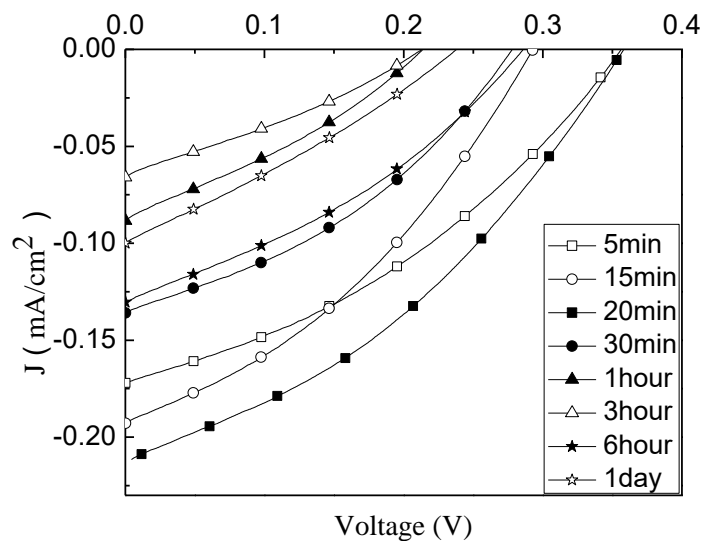
Figure (4.11): Current density (J) versus voltage (V) characteristic curves for DSSCs sensitized with Haematoxylin dye solutions at various dying times.
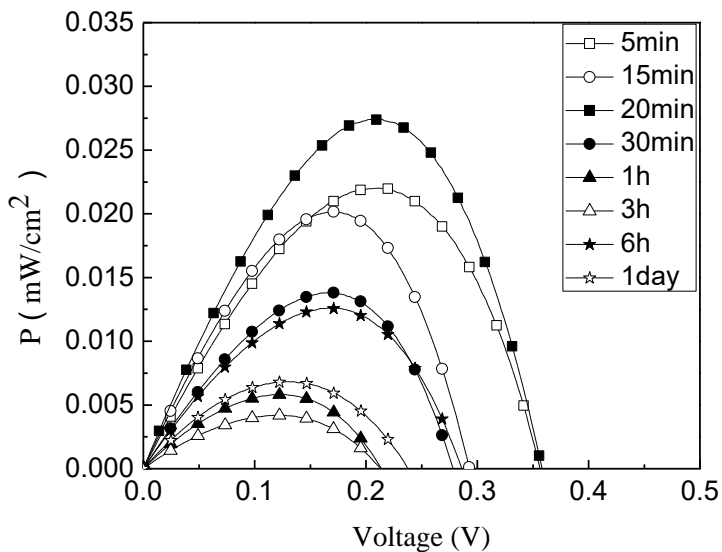
Figure (4.12): Power (P) versus voltage (V) characteristic curves for DSSCs sensitized with Haematoxylin dye solutions at various dying times.
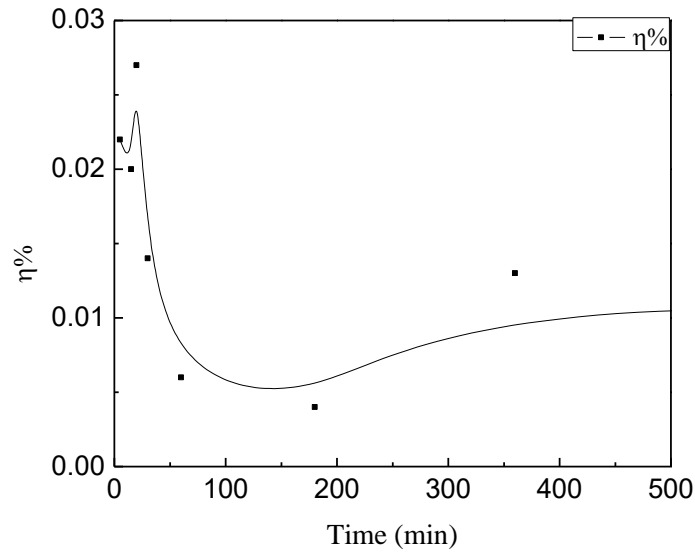
Figure (4.13): DSSC efficiency versus the dying time of the Haematoxylin dye solutions at various dying times.

Table (4. 2): Photovoltaic parameters of the DSSCs sensitized by Haematoxylin dye solutions at various dying times.

Dyeing time	J_{sc} (mA/cm^2)	V_{oc} (V)	J_m (mA/cm^2)	V_m (V)	P_{max} (mwatt/cm^2)	FF	η %
5 minute	0.17	0.36	0.10	0.21	0.022	0.35948	0.022
15 minute	0.19	0.29	0.12	0.17	0.020	0.36298	0.020
20 minute	0.21	0.36	0.13	0.21	0.027	0.35714	0.027
30 minute	0.14	0.28	0.08	0.17	0.014	0.35714	0.014
1 hour	0.09	0.21	0.05	0.12	0.006	0.31746	0.006
3 hour	0.06	0.21	0.03	0.12	0.004	0.31746	0.004
6 hour	0.13	0.29	0.07	0.17	0.013	0.34483	0.013
1 day	0.10	0.24	0.05	0.13	0.007	0.29167	0.007

4.5 Dye Uptake

Determination of the amount of haematoxylin dye adsorbed on the TiO_2 films in the assembled DSSCs was carried out by the desorption method.

In the DSSCs fabrication, the dying process has an essential impact on the final cell performance. Moreover, it is a critical step from the scale-up viewpoint. Usually adopted dye uptake measurements are based on dye desorption from photoanode after specified time intervals using a basic (i.e., NaOH or KOH) solution, and on the subsequent UV-Vis spectroscopy.

Experimental method to find the concentration of Haematoxylin dye in TiO_2 layer by using UV-Vis Spectroscopy can be summarized as follow

1. Prepared TiO_2 samples.
2. Dying samples by Haematoxylin dye for 20 minute.
3. Drying dyed samples by oven on 60^oC.
4. Putting samples in NaOH (0.1M) solution for one day.
5. Finding the absorbance of the NaOH and Haematoxylin dye solution about different concentration by UV-Vis Spectroscopy as shown in Figure (4.14).

It is found that the TiO_2 take $7 \times 10^{-6} molar$ from Haematoxylin dye, that means that it take only 0.7% from the dye.
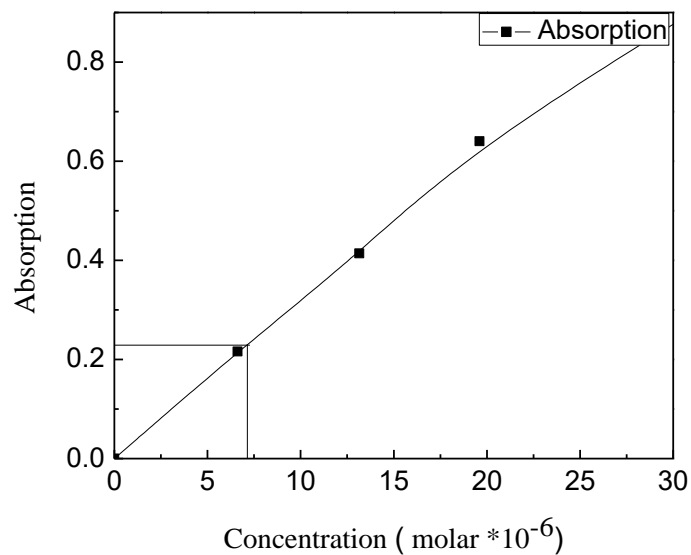
Figure (4.14): Absorption versus concentration (molar*10^{-6}) characteristic curves for Haematoxylin dye in DSSCs.

4.6 Effect of pH of Haematoxylin Dye Solution on DSSCs Efficiency

To investigate the effect of the pH of the dye solution on the performance of the DSSC sensitized by Haematoxylin dye as photosensitizer, the pH of the dye was changed with HCl and NaOH. The original pH of Haematoxylin dye in Ethanol was measured to be 5.7 using pH meter. Seven different pH values ranging from 2.9 to 8.8 were examined by adding 0.001M from HCl and NaOH to the dye solutions as shown in Figure (4.15).

Figure (4.15): Changing the pH of the Haematoxylin dye solutions using hydrochloric acid and sodium hydroxide.

The J-V characteristics of the DSSCs sensitized with Haematoxylin dye at different values of pH using HCl and NaOH are shown in Figure (4.16). Moreover, the power versus voltage for all DSSCs using the Haematoxylin dyes at different pH values is shown in Figure (4.17).

Figure (4.18) shows the DSSC efficiency as a function of the pH values of the extract solutions of Haematoxylin dye using hydrochloric acid and Sodium hydroxide. Table (4.3) shows the photovoltaic parameters of the DSSCs sensitized by Haematoxylin dye at different pH values using hydrochloric acid and sodium hydroxide. As observed from the figure (4.18), the efficiency is maximum when the PH value is 5.7 (without adding acid or base), and decreases when the value of PH increases or decreases.
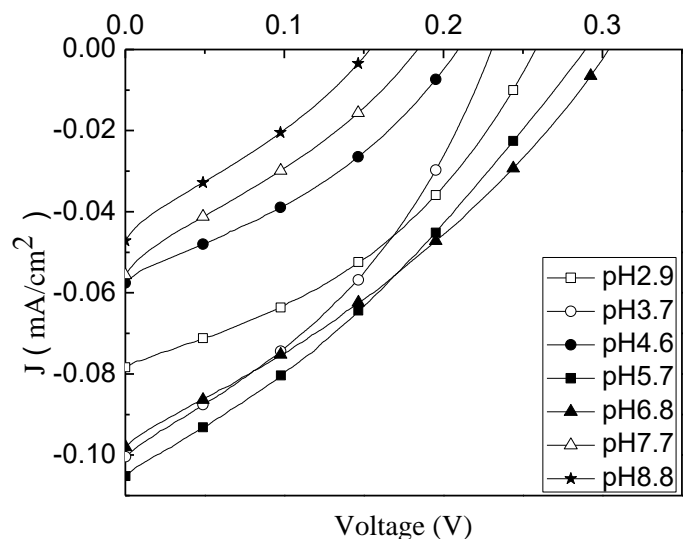
Figure (4.16): Current density (J) versus voltage (V) characteristic curves for DSSCs sensitized with Haematoxylin dye solutions at various pH values using hydrochloric acid and sodium hydroxide.
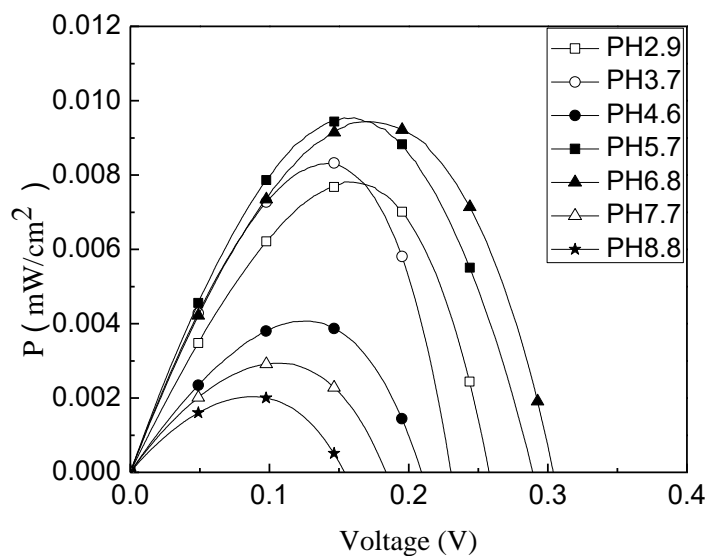
Figure (4.17): Power (P) versus voltage (V) characteristic curves for DSSC sensitized with Haematoxylin dye solutions of various pH values using hydrochloric acid and sodium hydroxide.
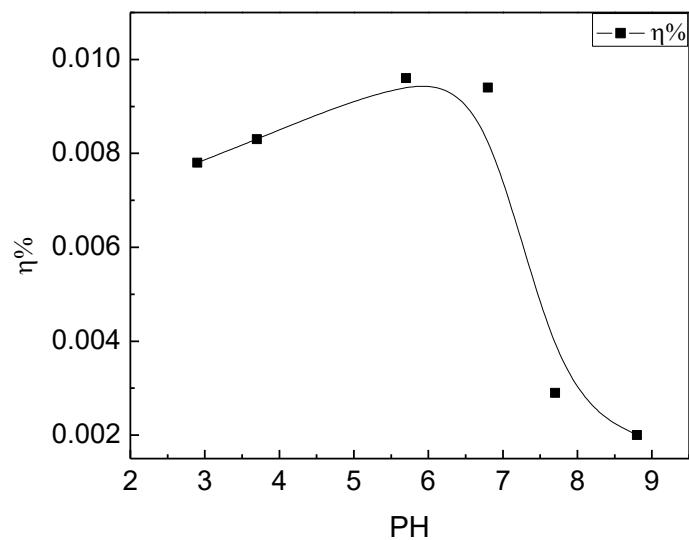
Figure (4.18): DSSC efficiency versus the pH of the Haematoxylin dye using hydrochloric acid and sodium hydroxide.

Table (4. 3): Photovoltaic parameters of the DSSCs sensitized by Haematoxylin dye at different pH vales using hydrochloric acid and sodium hydroxide.

PH	J_{sc} (mA/cm^2)	V_{oc} (V)	J_m (mA/cm^2)	V_m (V)	P_{max} (mwatt/cm^2)	FF	η %
2.9	0.08	0.26	0.048	0.16	0.0078	0.375	0.0078
3.7	0.10	0.23	0.059	0.14	0.0083	0.36087	0.0083
4.6	0.06	0.21	0.034	0.12	0.0041	0.3254	0.0041
5.7	0.11	0.29	0.058	0.16	0.0096	0.30094	0.0096
6.8	0.097	0.30	0.055	0.17	0.0094	0.32302	0.0094
7.7	0.055	0.18	0.026	0.11	0.0029	0.29293	0.0029
8.8	0.047	0.15	0.022	0.09	0.002	0.28369	0.002

4.7 Effect of adding copper and iron ions on haematoxylin dye

To investigate the effect of adding copper and iron ions with 0.1M concentration on the performance of Haematoxylin dye as a photosensitizer. The ions were added to the dye with the ratio 1:3 (16.7µl ions to 5ml haematoxylin). Dyes treated with cupric sulfate ($CuSO_4$) and ferrous sulfate ($FeSO_4$) dissolved in water and ethanol are shown in Figure (4.19). The I-V characteristics were then measured using redox (I^-/I^{-3}) electrolyte and using sodium carbonate (Na_2CO_3) with the redox with a concentration of 0.1M.

Figure (4.19): The treatment of the Haematoxylin dye solutions using cupric sulfate (CuSO4) and ferrous sulfate (FeSO4).

4.7.1 Effect of adding copper and iron ions with water solvent

The J-V characteristics of the DSSCs sensitized with Haematoxylin dye with copper and iron ions using water as a solvent are shown in Figure (4.20). It is worth mentioning that the (I^-/I^{-3}) electrolyte solution was used with these cells. The power with voltage curves of these cells are shown in Figure (4.21). When adding sodium carbonate (Na_2CO_3) to the redox and measuring the J-V curves; the results are illustrated in Figure (4.22). Moreover, the power with voltage for these cells are shown in Figure (4.23).

Tables (4.4) and (4.5) show the photovoltaic parameters of these DSSCs. As observed from Table (4.4), the highest efficiency was obtained when dissolving the Haematoxylin dye in water without adding ions. Table (4.5) shows that when using sodium carbonate (Na_2CO_3) with the electrolyte, there is an improvement of 115% in the efficiency of the cell when compared to the cell measured using the redox without Na_2CO_3. When adding copper ions, an improvement of 120% in the efficiency of the cell when compared to the cell measured using the redox without Na_2CO_3. And when adding ferrous ions, an improvement of 267% in the efficiency of the cell when compared to the cell measured using the redox without Na_2CO_3.

The abbreviations in Figures (4.20), (4.21), (4.22) and (4.23) are as follow:

❖ W: Haematoxylin dye dissolved in water and the measurements were
     performed using (I^-/I^{-3}) redox.

❖ Wx: Haematoxylin dye dissolved in water and the measurements were
     performed using (I^-/I^{-3}) redox with adding Na_2CO_3.

❖ Cu: Haematoxylin dye with copper ions dissolved in water and the
     measurements were performed using (I^-/I^{-3}) redox.

❖ Cux: Haematoxylin dye with copper ions dissolved in water and
     the measurements were performed using (I^-/I^{-3}) redox with Na_2CO_3.

47

❖ Fe: Haematoxylin dye with iron ions dissolved in water and the

      measurements were performed using (I^-/I^{-3}) redox.

❖ Fex**:** Haematoxylin dye with iron ions dissolved in water and

      the measurements were performed using (I^-/I^{-3}) redox with Na_2CO_3.

4.7.1.1 Measurements using redox (I^-/I^{-3}) electrolyte
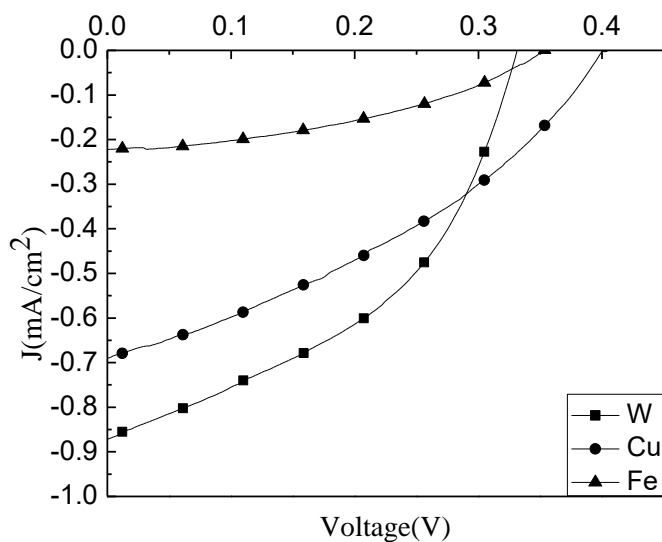
Figure (4.20): Current density (J) versus voltage (V) characteristic curves for DSSCs sensitized with Haematoxylin dye solutions with copper and iron ions using water as a solvent.
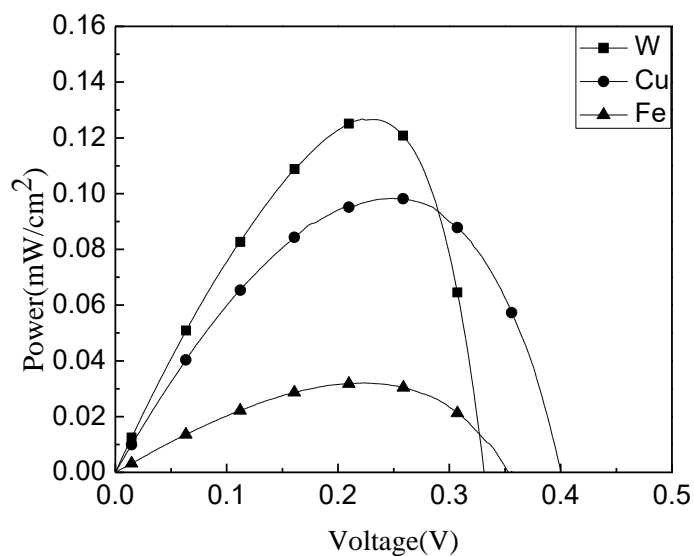
Figure (4. 21): Power (P) versus voltage (V) characteristic curves for DSSCs sensitized with Haematoxylin dye solutions with copper and iron ions using water as a solvent**.**

Table (4.4): Photovoltaic parameters of the DSSCs sensitized by Haematoxylin dye solutions with copper and iron ions using water as solvent.

Dye with	J_{sc} (mA/cm^2)	V_{oc} (V)	J_m (mA/cm^2)	V_m (V)	P_{max} (mwatt/cm^2)	FF	η %
W	0.87	0.33	0.55	0.23	0.13	0.4528	0.13
Cu	0.70	0.40	0.37	0.26	0.10	0.35714	0.10
Fe	0.22	0.35	0.14	0.22	0.03	0.38961	0.03

4.7.1.2 Measurements using redox (I^-/I^{-3}) electrolyte with sodium carbonate (Na_2CO_3)

Figure (4.22): Current density (J) versus voltage (V) characteristic curves for DSSCs sensitized with Haematoxylin dye solutions with copper and iron ions using water as solvent and measuring using redox with Na_2CO_3.
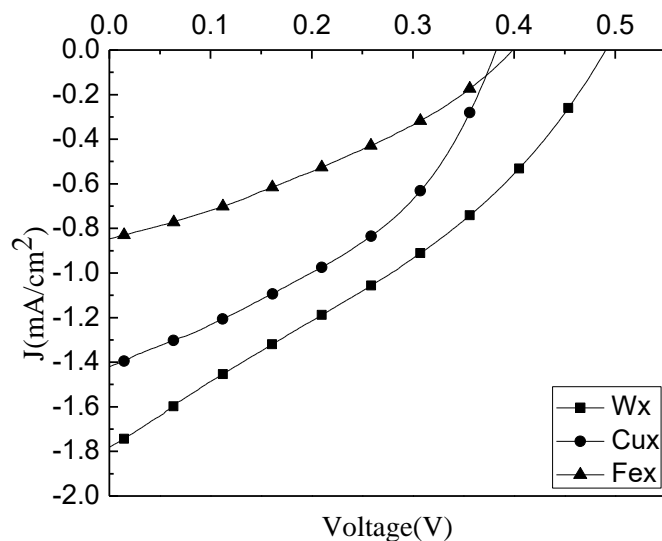
Figure (4. 23): Power (P) versus voltage (V) characteristic curves for DSSCs sensitized with Haematoxylin dye solutions with copper and iron ions using water as a solvent and measuring using redox with Na_2CO_3.
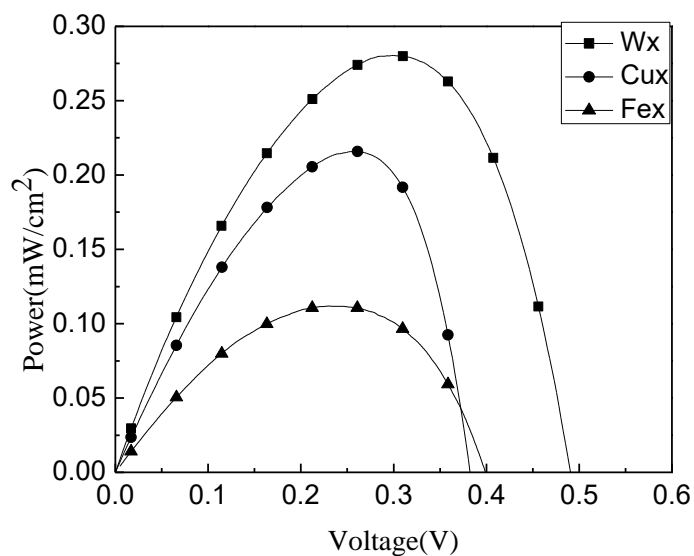
Table (4.5): Photovoltaic parameters of the DSSCs sensitized by Haematoxylin dye solutions with copper and iron ions using water as a solvent with adding Na_2CO_3 to the redox.

Dye with	J_{sc} (mA/cm^2)	V_{oc} (V)	J_m (mA/cm^2)	V_m (V)	P_{max} (mwatt/cm^2)	FF	η %
Wx	1.79	0.49	0.93	0.30	0.28	0.31923	0.28
Cux	1.43	0.38	0.82	0.26	0.22	0.40486	0.22
Fex	0.85	0.40	0.46	0.24	0.11	0.32353	0.11

4.7.2 Effect of adding copper and iron ions with ethanol solvent

The J-V characteristics of the DSSCs sensitized Haematoxylin dye with copper and iron ions using ethanol as a solvent are shown in Figure (4.24). It is worth mentioning that the (I^-/I^{-3}) electrolyte solution was used with these cells. The power with voltage curves of these cells are shown in Figure (4.25). When adding sodium carbonate (Na_2CO_3) to the redox and measuring the J-V curves; the results are illustrated in Figure (4.26). Moreover, the power with voltage for these cells are shown in Figure (4.27).

Tables (4.6) and (4.7) show the photovoltaic parameters of these DSSCs. As observed from Table (4.6), the highest efficiency was obtained when dissolved Haematoxylin dye in ethanol with iron ions by 0.14%. There is an improvement of 75% in the efficiency of the cell when compared to the cell measured using the redox without Na_2CO_3. When adding copper ions, an improvement of 233% in the efficiency of the cell when compared to the cell measured using the redox without Na_2CO_3. And when adding ferrous ions, an improvement of 43% in the efficiency of the cell when compared to the cell measured using the redox without Na_2CO_3.

The abbreviations in Figures (4.24), (4.25), (4.26) and (4.27) are as follow:

❖ E: Haematoxylin dye dissolved in ethanol and the measurements were
performed using (I^-/I^{-3}) redox.

❖ Ex: Haematoxylin dye dissolved in ethanol and the measurements were
performed using (I^-/I^{-3}) redox with Na_2CO_3.

❖ Cu: Haematoxylin dye with copper ions dissolved in ethanol and the
measurements were performed using (I^-/I^{-3}) redox.

❖ Cux: Haematoxylin dye with copper ions dissolved in ethanol and
the measurements were performed using (I^-/I^{-3}) redox with Na_2CO_3.

❖ Fe: Haematoxylin dye with iron ions dissolved in ethanol and the
measurements were performed using (I^-/I^{-3}) redox.

❖ **Fex:** Haematoxylin dye with iron ions dissolved in ethanol and
the measurements were performed using (I^-/I^{-3}) redox with Na_2CO_3.

4.7.2.1 Measured by redox (I^-/I^{-3}) electrolyte
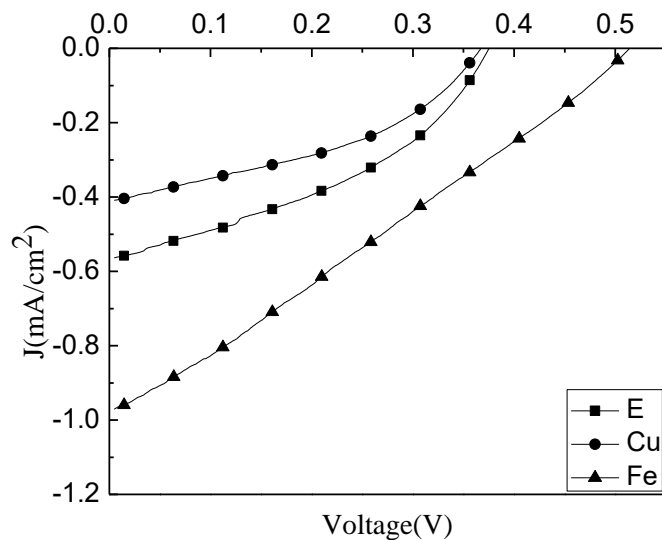
Figure (4.24): Current density (J) versus voltage (V) characteristic curves for DSSCs sensitized with Haematoxylin dye solutions with copper and iron ions using ethanol as a solvent.
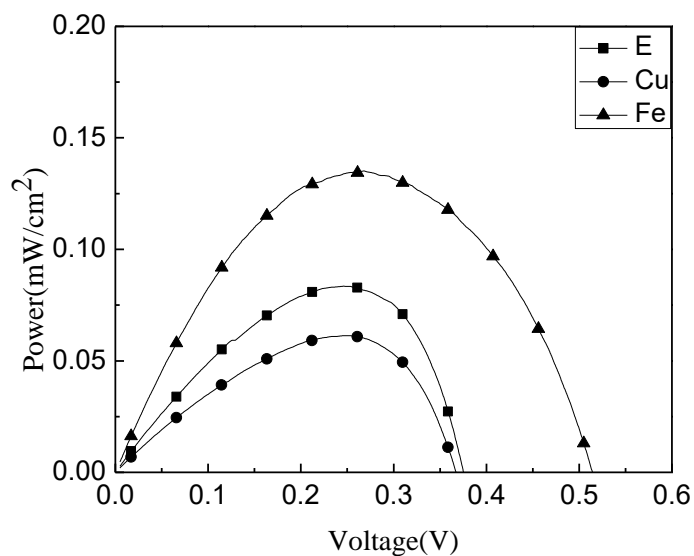
Figure (4.25): Power (P) versus voltage (V) characteristic curves for DSSCs sensitized with Haematoxylin dye solutions with copper and iron ions using ethanol as a solvent**.**

Table (4.6): Photovoltaic parameters of the DSSCs sensitized by Haematoxylin dye solutions with copper and iron ions using ethanol as a solvent.

Dye with	J_{sc} (mA/cm^2)	V_{oc} (V)	J_m (mA/cm^2)	V_m (V)	P_{max} (mwatt/cm^2)	FF	η %
E	0.58	0.38	0.33	0.25	0.08	0.36298	0.08
Cu	0.42	0.37	0.23	0.26	0.06	0.3861	0.06
Fe	0.98	0.51	0.50	0.27	0.14	0.28011	0.14

4.7.2.2 Measurements using redox (I^-/I^{-3}) electrolyte with sodium carbonate (Na_2CO_3)

Figure (4.26): Current density (J) versus voltage (V) characteristic curves for DSSCs sensitized with Haematoxylin dye solutions with copper and iron ions using ethanol as a solvent and measuring using redox with Na_2CO_3.

Figure (4. 27): Power (P) versus voltage (V) characteristic curves for DSSCs sensitized with Haematoxylin dye solutions with copper and iron ions using ethanol as a solvent and measuring using redox with Na_2CO_3.
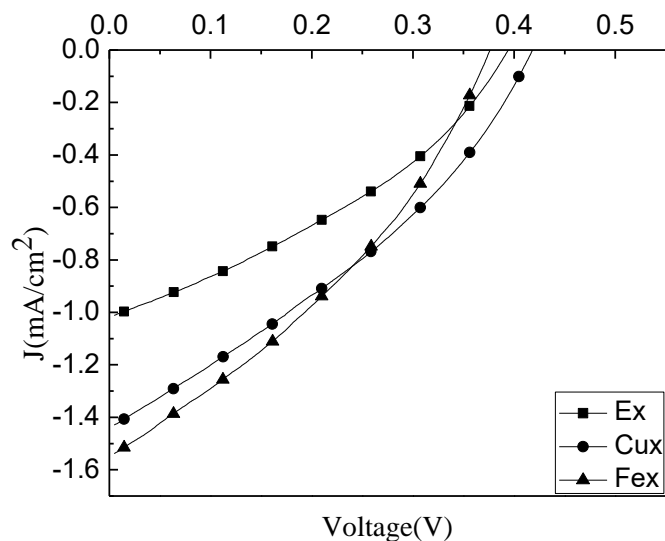
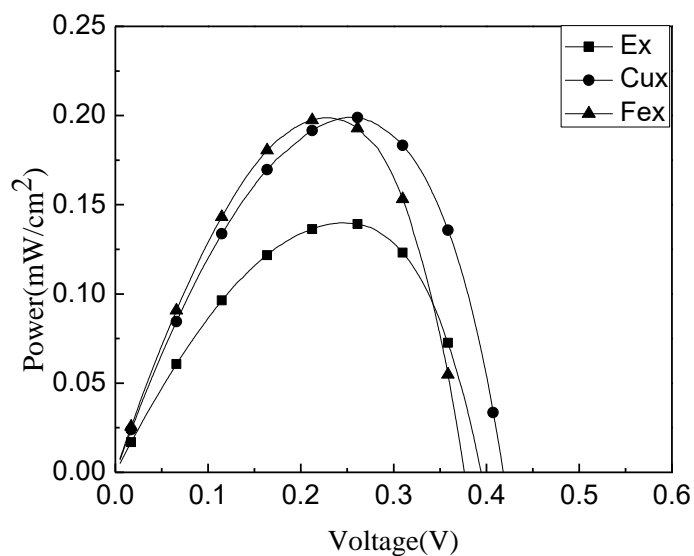**Table (4.7):** Photovoltaic parameters of the DSSCs sensitized by Haematoxylin dye solutions with copper and iron ions using ethanol as a solvent and measuring by redox with adding Na_2CO_3 to the redox.

Dye with	J_{sc} (mA/cm^2)	V_{oc} (V)	J_m (mA/cm^2)	V_m (V)	P_{max} (mwatt/cm^2)	FF	η %
Ex	1.03	0.40	0.55	0.25	0.14	0.33981	0.14
Cux	1.45	0.42	0.77	0.26	0.20	0.32841	0.20
Fex	1.56	0.38	0.86	0.23	0.20	0.33738	0.20

Finally, as observed from Tables (4.4), (4.5), (4.6) and (4.7), it is observed that the DSSCs exhibit better performance when using water as a solvent without adding ions. There is a considerable improvement in the DSSC efficiency when using Na_2CO_3 with the redox. When using ethanol as a solvent and adding ferrous ion, the efficiency showed an improvement.

Conclusion

Conclusion

The main aim of this work was to investigate the performance of DSSCs sensitized with haematoxylin dye and to study the effect of several treatments on the performance of these cells such as dying time, different pH of dye solution, adding copper and iron ions to the dye and effect of adding sodium carbonate to the redox.

The optical properties of haematoxylin dye solution were characterized using UV-Vis spectroscopy. The absorption spectrum of haematoxylin dye dissolved in ethanol and water showed a main peak at the same wavelength of 446 nm, and the absorption spectrum of the dye on TiO_2 (kubelka-munk) shows a shift towards higher wavelengths.

HOMO and LUMO energy levels were calculated by the cyclic voltammetry potentiostatic and found to be $-5.33\ eV$ and $-1.29\ eV$, respectively.

It was found that the TiO_2 take $7 \times 10^{-6} molar$ from Haematoxylin dye, which it takes only 0.7% from the dye.

The DSSCs sensitized with haematoxylin dye for 20 minutes were observed to have the best performance.

The results showed decreasing the efficiency of DSSCs sensitized with haematoxylin dye when adding HCl & NaOH to change the pH of the dye solution and a pH of 5.7 (normal) showed the best result.

The results showed increasing efficiency for DSSCs sensitized with haematoxylin dye using water as a solvent instead of ethanol. Moreover, the efficiency can be increased when adding the copper ions on the dye dissolved in water and when adding the ferrous ions on the dye dissolved in ethanol.

In addition, there is a remarkable improvement in the cell efficiency when adding sodium carbonate to the redox.

References

References

Abdel-Latif, M. S., Abuiriban, M. B., El-Agez, T. M., & Taya, S. A. (2015). Dye-sensitized solar cells using dyes extracted from flowers, leaves, parks, and roots of three trees. *International Journal of Renewable Energy Research, 5*(1), 294-298.

Asbury, J. B., Ellingson, R. J., Ghosh, H. N., Ferrere, S., Nozik, A. J., & Lian, T. (1999). Femtosecond IR study of excited-state relaxation and electron-injection dynamics of Ru (dcbpy) 2 (NCS) 2 in solution and on nanocrystalline TiO2 and Al2O3 thin films. *The Journal of Physical Chemistry B, 103*(16), 3110-3119.

Becquerel, A. (1839). Mémoire sur les effets électriques produits sous l'influence des rayons solaires. Comptes Rendus 9: 561–567. *Originalarbeit zur Einwirkung von Licht auf Elektroden*.

Britt, J., & Ferekides, C. (1993). Thin-film CdS/CdTe solar cell with 15.8% efficiency. *Applied physics letters, 62*(22), 2851-2852.

Corkish, R., Green, M. A., Watt, M. E., & Wenham, S. R. (2013). *Applied photovoltaics*: Routledge.

Cotal, H., Fetzer, C., Boisvert, J., Kinsey, G., King, R., Hebert, P., . . . Karam, N. (2009). III–V multijunction solar cells for concentrating photovoltaics. *Energy & Environmental Science, 2*(2), 174-192.

Dye-sensitized solar cells: Best energy harvesting sources for future AF UAVs.
Retrieved from
http://www.labspaces.net/98621/Dye_sensitized_solar_cells__Best_energy_harv
esting_sources_for_future_AF_UAVs

Forrest, S. R. (2005). The limits to organic photovoltaic cell efficiency. *MRS bulletin, 30*(01), 28-32.

Grätzel, M. (2005). Solar energy conversion by dye-sensitized photovoltaic cells. *Inorganic chemistry, 44*(20), 6841-6851.

Green, M. A., Emery, K., Hishikawa, Y., Warta, W., & Dunlop, E. D. (2013). Solar cell efficiency tables (version 42). *Progress in photovoltaics: research and applications, 21*(5), 827-837.

GREENY, M. A., Emery, K., Hishikawa, Y., & Warta, W. (2011). Solar cell efficiency tables (version 37). *Progress in photovoltaics, 19*(1), 84-92.

Halme, J. (2002). Dye-sensitized nanostructured and organic photovoltaic cells: technical review and preliminary tests. *Master of Science in Technology, Helsinki University of Technology, Helsinki, Finland.*

Jones, A., Verlinden, N., & Quimby, R. (2007). Optical properties of quantum dots: An undergraduate Physics Laboratory.

Luque, A., & Hegedus, S. (2011). *Handbook of photovoltaic science and engineering*: John Wiley & Sons.

Meyer-Arendt, J. R. (1989). Introduction to classical and modern optics. *Englewood Cliffs: Prentice-Hall, 1989, 3rd ed.*

Nelson, J. (2003). *The physics of solar cells*: World Scientific Publishing Co Inc.

Rouessac, F., & Rouessac, A. (2013). *Chemical analysis: modern instrumentation methods and techniques*: John Wiley & Sons.

Stanley, A., Verity, B., & Matthews, D. (1998). Minimizing the dark current at the dye-sensitized TiO 2 electrode. *Solar Energy Materials and Solar Cells, 52*(1), 141-154.

Toivola, M. (2010). Dye-sensitized solar cells on alternative substrates.

Upadhyaya, H. M., Senthilarasu, S., Hsu, M.-H., & Kumar, D. K. (2013). Recent progress and the status of dye-sensitised solar cell (DSSC) technology with state-of-the-art conversion efficiencies. *Solar Energy Materials and Solar Cells, 119*, 291-295.

Winter, C.-J., Sizmann, R. L., & Vant-Hull, L. L. (2012). *Solar power plants: fundamentals, technology, systems, economics*: Springer Science & Business Media.

Wolfbauer, G. (1999). The electrochemistry of dye sensitised solar cells, their sensitisers and their redox shuttles. *Departmen of Chemistry*.

Wolfbauer, G., Bond, A. M., Eklund, J. C., & MacFarlane, D. R. (2001). A channel flow cell system specifically designed to test the efficiency of redox shuttles in dye sensitized solar cells. *Solar Energy Materials and Solar Cells, 70*(1), 85-101.

Zghal, W., Kantchev, G., & Kchaou, H. (2012). *Determination of the exploitable solar energy for electricity generation using the photovoltaic systems.* Paper presented at the Renewable Energies and Vehicular Technology (REVET), 2012 First International Conference on.